EFFECTS OF THE ANTHROPOGENIC LANDSCAPE ON GLOBAL SCALE SUSPENDED SEDIMENT FLUX

by

SHAWN M. CARTER

SAGY COHEN, COMMITTEE CHAIR
EBEN BROADBENT
ALBERT KETTNER

A THESIS

Submitted in partial fulfillment of the requirements
for the degree of Master of Science
in the Department of Geography
in the Graduate School of
The University of Alabama

TUSCALOOSA, ALABAMA

2016

ABSTRACT

Human industry and agriculture have long-term effects on the erosion and transport of sediment from the continental surface to the ocean. Riverine suspended sediment flux can be increased where soils are exposed to erosion but can also be trapped behind reservoirs or under impervious surfaces. Literature examining the effects of anthropogenic land-use and disturbance on suspended sediment flux are generally limited to individual reaches, streams, or basins. This thesis describes and analyzes the first global-scale and spatially-explicit model simulating the effect of anthropogenic land-use on suspended sediment flux.

Quantifying suspended sediment flux at the global scale is complicated by the limited extent of gaging stations and observed datasets. Modeling provides a pathway for researchers to investigate the flux of sediment from the terrestrial environment to the coastal ocean where there is a lack of observed records. Anthropogenic land-use effects on global suspended sediment flux are investigated here by incorporating a new spatially and temporally explicit parameter in the WBMsed model, a global-scale riverine modeling framework.

A new anthropogenic factor (A_d) is developed and validated for the WBMsed model. A_d is created from readily available and regularly updated land-use/land-cover datasets and used to calculate the effect of land-use in a spatially and temporally explicit manner. The results of the model validation show that incorporating A_d into WBMsed increases intra-basin variability of suspended sediment flux predictions. The A_d parameter also has the effect of increasing the model's relative accuracy with observed long-term suspended sediment records in streams with smaller drainage areas.

Following the validation of the A_d factor in WBMsed, we analyze the anthropogenic contribution to global suspended sediment flux. Our results show that although anthropogenic disturbance increases overall suspended sediment flux on every continent, this signal is masked by the mitigating effect of reservoir trapping of sediment. By isolating sediment trapping and land-use effects, the global-scale, spatially-explicit quantification of anthropogenically contributed suspended sediment is provided.

LIST OF ABBREVIATIONS AND SYMBOLS

A upstream basin area (km^2).

A_d dimensionless category combining E_h and A_d.

A_n percentage of agricultural land-use within a basin.

array A list of values identified by a numeric value.

B dimensionless term accounting for human and geological factors..

E_h dimensionless category of socioeconomic factors.

L dimensionless category describing relative resistance to erosion of basin bedrocks.

MODIS Moderate Resolution Imaging Spectroradiometer.

Q stream discharge ($m^3\ s^{-1}$).

R basin relief (km).

SPARROW Spatially Referenced Regression on Watershed attributes.

T mean basin air temperature (C°).

T_e dimensionless category describing the trapping efficiency of reservoirs.

USGS United States Geological Survey.

WBMsed Water Balance Model (Sediment Flux).

WEPP Water Erosion Prediction Program.

ACKNOWLEDGMENTS

Many thanks to my committee chair, Dr. Sagy Cohen. Without his guidance, wisdom, and patience this thesis would have been impossible. I also owe a debt of gratitude to my committee members for their probing questions which tested my knowledge and truly prepared me to enter science as a profession. Most of all, I thank Lynn for her patience and understanding. You are more than my wife, you are my best friend and most trusted counselor. Your belief saw me through my own self-doubts. Without you, none of this would be possible.

CONTENTS

LIST OF TABLES

LIST OF FIGURES

CHAPTER 1

INTRODUCTION

Since historical periods, it has been known that farming, deforestation, and other activities on the landscape compact, pulverize, and otherwise expose soils to the elements which causes increased soil erosion (Dotterweich, 2013). The primary physical factors contributing to soil erosion include slope, precipitation, soil type, and land-cover (Kirkby, 1980; Hartanto et al., 2003; Syvitski and Milliman, 2007; Caitcheon et al., 2012). Land-cover affects surface friction on runoff which can inhibit or promote erosion and transport (Kasai et al., 2005). Kirkby (1980) explained that in a semi-arid region with little ground cover, increased precipitation following climate change would initially increase soil erosion by increasing runoff. However, the increase in precipitation will lead to an increase in vegetation growth resulting in reduced soil loss over the long-term. Plants inhibit soil erosion by reducing the kinetic energy of rainfall to disassociate soil grains or cause soil crusting (Walker et al., 2007). With all factors equal, vegetation, or more accurately, lack of vegetation, has the most significant effect on soil erosion from precipitation and runoff (Kirkby, 1980).

Land-use is incorporated as an explanatory parameter in several sediment and soil erosion models. Importantly, land-use is not used as a single factor in most models but rather, in conjunction with land-use/cropping management styles which affect the mechanism and intensity of soil erosion as well as the spatial extent of the disturbance. Models that we review here approach land-use and land-use management as empirical factors or physically based simulations. The common thread between all the models, is that anthropogenic land-use is a contributing parameter increasing soil erosion in the modeled environment.

Agriculture exacerbates soil erosion by replacing perennial native vegetation with short-lived species and exposing soil to erosive elements. Agricultural practices can also compact and pulverize soil decreasing the soil's cohesion and resistance to erosion (Dotterweich, 2013). Using the Water Erosion Prediction Program (WEPP), Maalim et al. (2013) demonstrated that modern soil erosion and sediment yield in the Le Seueur Watershed of Minnesota is far greater than the amounts prior to the arrival of European settlers (Table 1.1), even though runoff depth had not significantly changed. Maalim et al. (2013) also found that the method of agriculture was an important factor controlling sediment yield; traditional methods (row cropping with fall tillage) in corn and soybean fields generated >20% more soil erosion than fields managed with no-till cropping methods.

Table 1.1: Effect of different land-use scenarios on WEPP simulations. Scenario 1 conventional agriculture, Scenario 2 no-till agriculture, Scenario 3 Pre-settlement (no agriculture) (Maalim et al., 2013)

	Land-use/Land-Cover	Average runoff depth (mm)	Runoff coefficient (%)	Average soil loss (T/ha)	Average sediment yield (T/ha)	Sediment delivery ratio (%)
Scenario 1	Agriculture	85.0	0.099	2.72	2.29	84.1
	Forest	99.8	0.117	0.63	0.53	83.0
	Urban/Developed	211.4	0.247	3.53	3.43	97.4
	Grass	77.0	0.090	0.12	0.09	72.9
Scenario 2	Agriculture	72.3	0.084	0.52	0.46	87.8
	Forest	97.5	0.114	0.69	0.57	83.6
	Urban/Developed	200.6	0.234	3.57	3.49	97.8
	Grass	66.5	0.078	0.12	0.09	72.8
Scenario 3	Forest	91.9	0.107	0.05	0.04	83.2
	Grass	74.9	0.087	0.42	0.29	68.6
	Prairie	70.0	0.082	0.20	0.14	72.8

The WEPP hillslope model simulates hillslope erosion and deposition by characterizing physical processes of soil erosion such as "infiltration, runoff, raindrop and flow detachment, sediment transport, deposition, plant growth, and residue decomposition" (Flanagan et al., 2007). It models both rill and interill erosion processes and computes

zones of deposition where sediment load exceeds sediment transport capacity. The WEPP watershed model, an extension of the WEPP hillslope model, was developed to model and predict erosion associated with different agricultural management practices, variability in topography, and soil characteristics within small watersheds (Flanagan et al., 1995). The model is limited to catchment areas <260 hectares (Flanagan et al., 2007), however, the importance of vegetative cover and agricultural management practices in the model's simulation is important insight for this study.

Another model which calculates long-term soil erosion is the Universal Soil Loss Equation and Revised Universal Soil Loss Equation (USLE/RUSLE). It is perhaps the most widely applied soil erosion model in the United Sates (Kirkby, 1980). It was developed by the United States Department of Agriculture following the devastation of the Dust Bowl in the 1930s and its intent is to guide soil conservationists implementing soil conservation programs in agricultural areas (Wischmeier and Smith, 1978). USLE/RUSLE is designed to estimate the long-term average annual soil loss in mass per unit area from interill and gully erosion on agricultural land. Published in 1965, the USLE is defined as $A = R * K * L * S * C * P$ where:

A = computed soil loss per unit area

R = rainfall erosivity

K = soil erodibility factor

L = slope length factor

S = slope gradient factor

C = cropping management factor

P = erosion control practices factor (Wischmeier and Smith, 1965)

USLE is limited to modeling soil erosion in agricultural lands and has no component describing transport of sediment into streams. Although USLE has limited utility for global scale soil erosion modeling, it is important to note the significance of land management practices found in Factor (P) and cropping management in Factor (C). USLE

was modified for use in other regions around the world (Stolpe, 2005) but there is not yet a single model appropriate for larger scale applications. Unlike the physically based WEPP model, USLE/RUSLE is an empirically based model; although these models are soil erosion models that have limited ability to predict suspended sediment, they were incorporated into this study because they predict soil erosion in a manner very similar to the BQART model's method of predicting suspended sediment flux.

The United States Geological Survey (USGS) Spatially Referenced Regression on Watershed attributes (SPARROW) model for suspended sediment concentrations of the contiguous United States incorporates land-cover and a modified version of RUSLE (USGS, 2008). Unlike WEPP and USLE/RUSLE, SPARROW does not incorporate land management practices. The coefficients for land-use contribution to suspended sediment loads (Table: 1.2) were derived from regression calculations of almost 2,000 long-term sediment monitoring stations operated between 1975-2007 with associated natural and anthropogenic basin characteristics (Roman et al., 2012).

The initial goal of the SPARROW project was to create a single national multivariate regression model to estimate suspended sediment discharge. However, initial models did not perform adequately ($R^2 = 0.64$) and the model was then re-calculated for each of the USGS Water Resource Regions achieving prediction R^2 values ranging from 0.76 to 0.93. Part of the difficulty in creating a single model for the conterminous United States was variability in the explanatory variables (e.g. Region 1 suspended sediment correlated with basin area and agricultural land-use area but Region 3 required different variables such as average May precipitation and soil permeability) (Roman et al., 2012)

Table 1.2: SPARROW land-class coefficients (From: USGS, 2008)

SPARROW Land Class Coefficients			
Land Class	*Estimate (kg/km^2/yr)*	*Standard Error*	*p-value*
Urban Land	47,130	9,925	0.000
Forested Land	634	898	0.480
Federal Non-Forested Land	63,344	12,411	0.000
Agricultural Land	18,047	3,623	0.000
Other Land	11,343	3,186	0.000
Streambed (reach length)	28.80 (kg/m/yr)	6.40	0.000

The regression analysis conducted by the USGS in developing the SPARROW model emphasizes the difficulty of tying land-use to suspended sediment flux at large scales. Land-use and suspended sediment have also been studied in China with similar findings demonstrating that the scale of the study is an important factor when trying to establish land-use as an explanatory factor of suspended sediment (Zhou et al., 2012). USLE/RUSLE, WEPP, and SPARROW are just a few of the many models that have been built to investigate soil erosion and sediment load processes and in one form or another, all three incorporate land-use as a determining factor while USLE/RUSLE and WEPP explicitly parameterize land management practices as well.

The BQART model was developed to quantify the geological, climatic, and anthropogenic factors in river basins which control the delivery of terrestrial sediment to the coastal ocean (Syvitski and Milliman, 2007). The model is a semi-empirical model developed from the basin characteristics and suspended sediment discharge of 294 river basins in the Milliman & Syvitski database (M&S92+) and validated against the 488 river basins in the Milliman & Farnsworth database (M&F05). M&F05 contains rivers that are smaller than those found in the M&S92+ database. The two databases account for 63% of the global land surface and 66% of the predicted global sediment load (Syvitski and Milliman, 2007).

The BQART model is defined as:

$$Q_s = \omega B Q^{0.31} A^{0.5} RT \ for \ T \geq 2°C \tag{1.1a}$$

$$Q_s = \omega B Q^{0.31} A^{0.5} R \ for \ T < 2°C \tag{1.1b}$$

where Q_s is in dimensions [M/T] with ω=0.02 for units of kg s^{-1}, or $\omega = 0.0006$ for units MT yr^{-1}, Q is discharge in km^3 yr^{-1}, A is basin area in km^2, R is basin relief in km, and T is mean basin air temperature in °C.

The B parameter of the BQART model is defined as:

$$B = IL(1 - T_e)E_h \tag{1.2}$$

where I is a parameter describing the amount of glaciated area in the river basin and has a range [1,10] corresponding to 0-100% ice cover, L describes erodobility of bedrock in the basin and has range [0.5, 2], T_e describes the sediment trapping efficiency of reservoirs formed behind impoundments range [0,1], and E_h is the anthropogenic factor which is created as a function of GNP per capita and population density. E_h is defined as:

$E_h = 0.3$ in basins where population density (PD) >200 km^{-2} and GNP >\$20k yr^{-1}.

$E_h = 1$ in basins where population density (PD) <50 km^{-2}.

$E_h = 2$ in basins where population density (PD) >200 km^{-2} and GNP ≤\$2.5k yr^{-1}.

The E_h parameter is predicated on the assumption that dense populations in poor areas have neither the motivation nor ability to establish and maintain soil conservation methods (Syvitski and Milliman, 2007). In these areas, the E_h parameter increases sediment flux in the BQART equation, whereas, in places with wealthier, densely populated areas, streams are assumed to be culverted and/or the extent of impervious surfaces limit the amount of sediment available for erosion. The E_h parameter is not a spatially explicit parameter and Syvitski and Milliman (2007) declared it as a "broad-brush, albeit a priori, approach".

When validated against the M&F05 database, the BQART model explained 94% of observed suspended sediment flux variability. The BQART model performed similarly against the M&S92+ database explaining the 95% of suspended sediment flux variability. The model demonstrated a mean bias of 3% when compared against the combined databases (Syvitski and Milliman, 2007). The BQART model proved to be well suited for calculating the long-term suspended sediment flux in large rivers. Cohen et al. (2013) would use the BQART equation as the starting point in developing the WBMsed global suspended sediment flux model.

WBMsed is a spatially and temporally explicit suspended sediment flux model (pixel scale and daily time-step) which calculates the BQART equation at each pixel; treating each pixel as the outlet of the drainage area above it (Cohen et al., 2013). WBMsed is a module in the WBMplus framework (Wisser et al., 2010) coupling the BQART and Psi variability models (Cohen et al., 2013). Following Kettner and Syvitski (2008) in the development of the HydroSHEDS model, WBMsed uses the Psi model (Morehead et al., 2003) to simulate daily suspended sediment flux simulations (Cohen et al., 2013) based on long-term BQART predictions.

The results of WBMsed sediment flux simulations were moderately correlated with the M&F05 database with an $R^2 = 0.66$ (Cohen et al., 2013). The apparent loss of suspended sediment prediction performance when comparing the correlation difference between the BQART model and WBMsed simulations likely stem from WBMsed's explicit calculations of BQART's dynamic parameters (e.g.$L,\ T_e,\ E_h$) (Cohen et al., 2013). BQART was designed to calculate suspended sediment flux at river mouths, but within WBMsed the BQART equation is being applied for every pixel in the model's input files.

When BQART is analyzed as a conceptual model, the E_h parameter (eq: 1.2) acts not unlike the C and P parameters in USLE/RUSLE. In essence, E_h describes the so-

cioeconomic ability to establish and manage land development and agricultural practices. Socioeconomic conditions are the controlling conditions of anthropogenically generated global sediment flux (Latrubesse et al., 2005). In order to modify the E_h parameter to be more spatially and temporally explicit, land-use must be considered. WBMsed currently runs at 6 arc-minute resolution (average 11km x 11km grid cells) and appropriate land-use classes are those that can be appreciably measured at that scale. Although forestry and mining both greatly disturb soil and are sources of amplified suspended sediment, the areal and temporal scale of the disturbance associated with those activities limits their applicability for this study (Hartanto et al., 2003; Walling, 2006). Agriculture, however, is a universal land-use which is easily detectable from remote sensing, is generally large-scale and long-term, and is a major contributor to soil erosion and sediment flux (Hoffmann et al., 2010).

A new land-use parameter (A_d) is developed to describe the spatial extent of socioeconomic conditions described in the E_h parameter. A_d is the result of a function between E_h and percent of upstream agricultural land-use (A_n). A_n is derived annual land-use datasets derived from satellite remote sensing. WBMsed with the incorporation of the A_d parameter is validated against a subset of the M&S92+ database and USGS streamgage data.

CHAPTER 2

METHODOLOGY

2.1 Developing the A_d Parameter

Global agricultural land-use was quantified using the Moderate Resolution Imaging Spectroradiometer (MODIS) land-use/land-cover data (MCD12Q1) (http://lpdaac.usgs.gov). MCD12Q1 data is freely available from the Land Processes Distributed Active Archive Center as a Level 3 MODIS product (Friedl et al., 2010). MCD12Q1 offers the advantage of quantifying land-use conversion and change at an annual time-step. Although there are five land-use/land-class data themes available with MCD12Q1, the International Geosphere-Biosphere Programme (IGBP) theme was used to develop the A_n variable because it categorizes the most land-classes. The MCD12Q1 IGBP data is produced annually at a 500-meter scale and characterizes land-use with 11 natural vegetation classes, three developed and mosaic land-classes, and three non-vegetated land classes (Friedl et al., 2010).

To create the A_n input files for WBMsed, we pre-process the MCD12Q1 datasets to extract the agricultural land-use information into a new binary raster (cells with a value of 1 indicate presence of an agricultural land-use and 0 indicates absence of agricultural land-use). A vector grid is created with the same dimensions as the WBMsed input data which is used to calculate zonal statistics of the agricultural land-use raster data. Following the zonal statistics operation, the vector grid contains the sum of the number of 500-meter land-use cells classified as agricultural in each 6 arc-minute grid. These sums are divided by the number of total possible cells to generate a percentage of agricultural land in each 6 arc-minute cell. The vector data is then rasterized and used as the weight value for a global flow accumulation analysis (Figure: 2.1). The flow accumulation anal-

ysis calculates the percentage of basin land classified as agricultural for each pixel. At this point, the agricultural land-use data is transformed into the A_n variable.

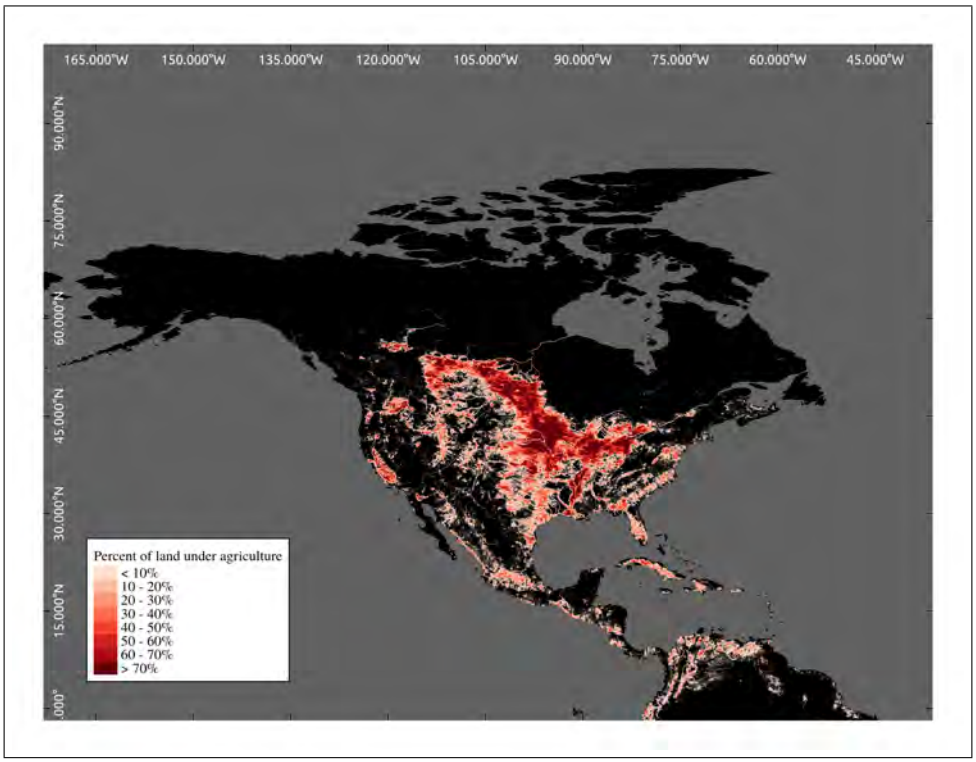

Figure 2.1: Sample of mean agricultural land (A_n) derived from MODIS MCD12Q1 data.

When sediment flux values from locations in the M&S92+ database are regressed against A_n, land-use is an insignificant factor in determining sediment flux (Figure: 2.2). This led to the conclusion that A_n cannot be used as a discrete parameter in the model. This is consistent with Vanmaercke et al. (2014) and is likely due to the heterogeneity in both intra- and inter-basin comparisons of both socioeconomic conditions and agricultural land-use contributions to suspended sediment flux (Hunter and Walton, 2008). A new parameter (A_d) is therefore developed that incorporates both socioeconomic (E_h) and land-use characteristics (A_n).

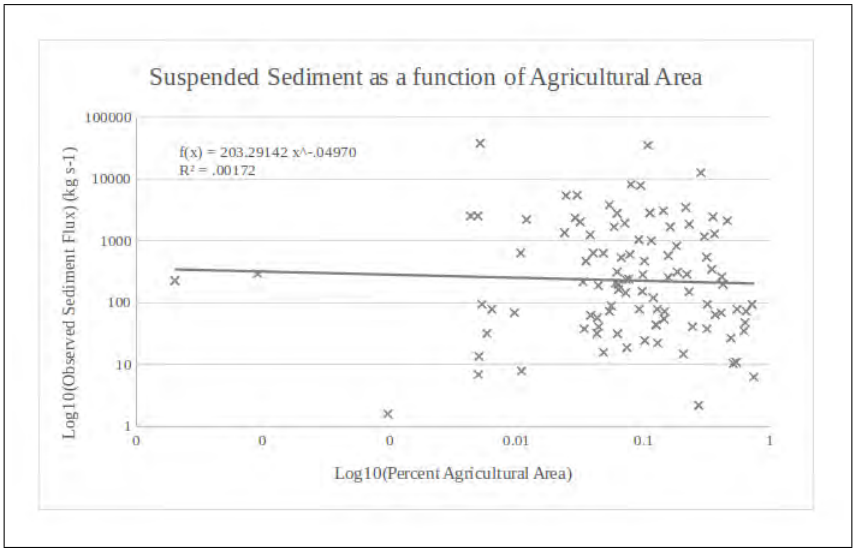

Figure 2.2: A_n as a function of observed suspended sediment discharge from the M&S92+ database.

Recognizing that agricultural land-use will impact suspended sediment flux variably due to differences in cropping styles and management practices, we followed the semi-empirical method used by Syvitski and Milliman (2007) by developing four equations for A_d based on assumptions of how agricultural land-use could alter the erosion rates and suspended sediment flux by combining E_h and A_d (Figure: 2.3). A function that strongly effected A_d with increasing A_n values was desired, but had to be balanced by the need to avoid overwhelming the model by increasing sediment by orders of magnitude. The objective was to give the E_h variable a spatial context, not necessarily increase overall predicted sediment quantities in the model. In other words, we sought to create a more realistic suspended sediment flux predictions that possessed more intra-basin and inter-basin dynamics. The following functions were incorporated into the BQART equation and tested against the M&S92+ database to determine which had the desired effect on

predicted suspended sediment:

$$A_d = E_h + A_n{}^{E_h} \tag{2.1a}$$

$$A_d = E_h * (10 * A_n) \tag{2.1b}$$

$$A_d = 10 * A_n^{\frac{1}{E_h}} \tag{2.1c}$$

$$A_d = E_h + A_n^{\frac{1}{E_h}} \tag{2.1d}$$

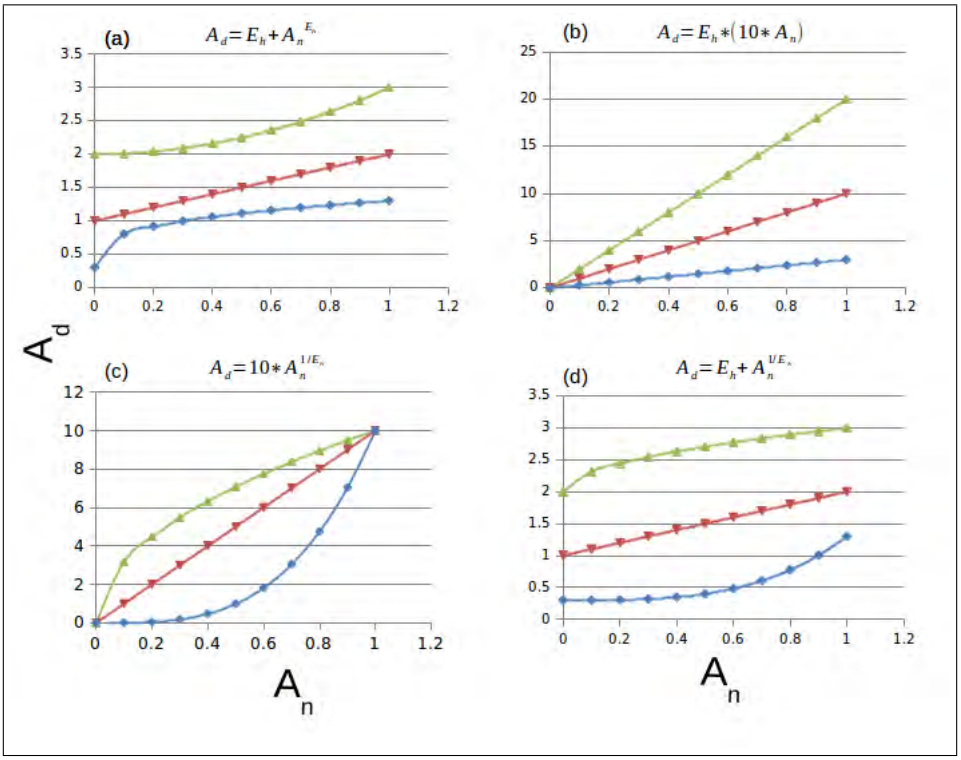

Figure 2.3: A_d response to increasing A_n.

Equation: 2.1a increases the impact of socioeconomic and land-use on suspended sediment flux non-linearly (Figure: 2.3 (a)). This equation was generated with the hypothesis that small areas of agriculture would have a limited effect on suspended sediment. As the percentage of A_n increases, A_d remains relatively stable until A_n is greater than ~20%. After which, the value of A_d accelerates moderately but is limited to increasing the overall B value to 100% greater than when calculated with the E_h parameter alone.

(Equation: 2.1a) With this equation, areas where E_h=0.3, small amounts of agricul-

tural land would greatly increase the predicted suspended sediment which counters the mitigating effect of E_h values below 1. Equation: 2.1b is a linear response function which increases the B parameter by orders of magnitude with small increases in A_n (Figure: 2.3 (b)). This equation would be applicable for regions that are sensitive to small disturbances. For example, areas that have recently been converted from forest and are situated on erodible soils and/or steep slopes. Equation: 2.1c is unique among the developed functions having a constant for the base instead of the E_h parameter. This function assumes that a basin with 100% agricultural land cover will create 10x more suspended sediment regardless of socioeconomic conditions (Figure: 2.3 (c)). This equation was developed by hypothesizing that anthropogenic impact can only increase suspended sediment flux by one order of magnitude. The final equation (Equation: 2.1d) is the mirror image to Equation: 2.1a. The value of A_d rapidly increases until A_n is equal to $\sim$20% after which increasing values of A_n gradually increase the value of A_d (Figure: 2.3 (d)). The maximum values for Equation: 2.1a and 2.1d are the same at 100% A_n. The equation was developed by hypothesizing that small amounts of anthropogenic land-use would produce much more suspended sediment over pristine conditions but as area increases there is less connectivity between land-use and stream channels. In other words, most of the eroded soil would be deposited on the landscape.

It can be expected that different equations for A_d will perform better in different regions or under different conditions. Indeed, the various equations presented could be applied in a spatially distributed manner to account for the spatial variability inherent in anthropogenic land-use's role in soil erosion (Hunter and Walton, 2008; Syvitski and Milliman, 2007), however in this study a universal equation is developed. The BQART equation was re-calculated using equations: 2.1a - 2.1d in the place of E_h. The resultant BQART R^2 against the M&S92+ database with the different A_d equations ranged from 0.94 to 0.42 (original BQART equation R^2=0.95). Equation 2.1d most similarly replicated the original BQART equation's accuracy and was therefore incorporated into the WBMsed source code.

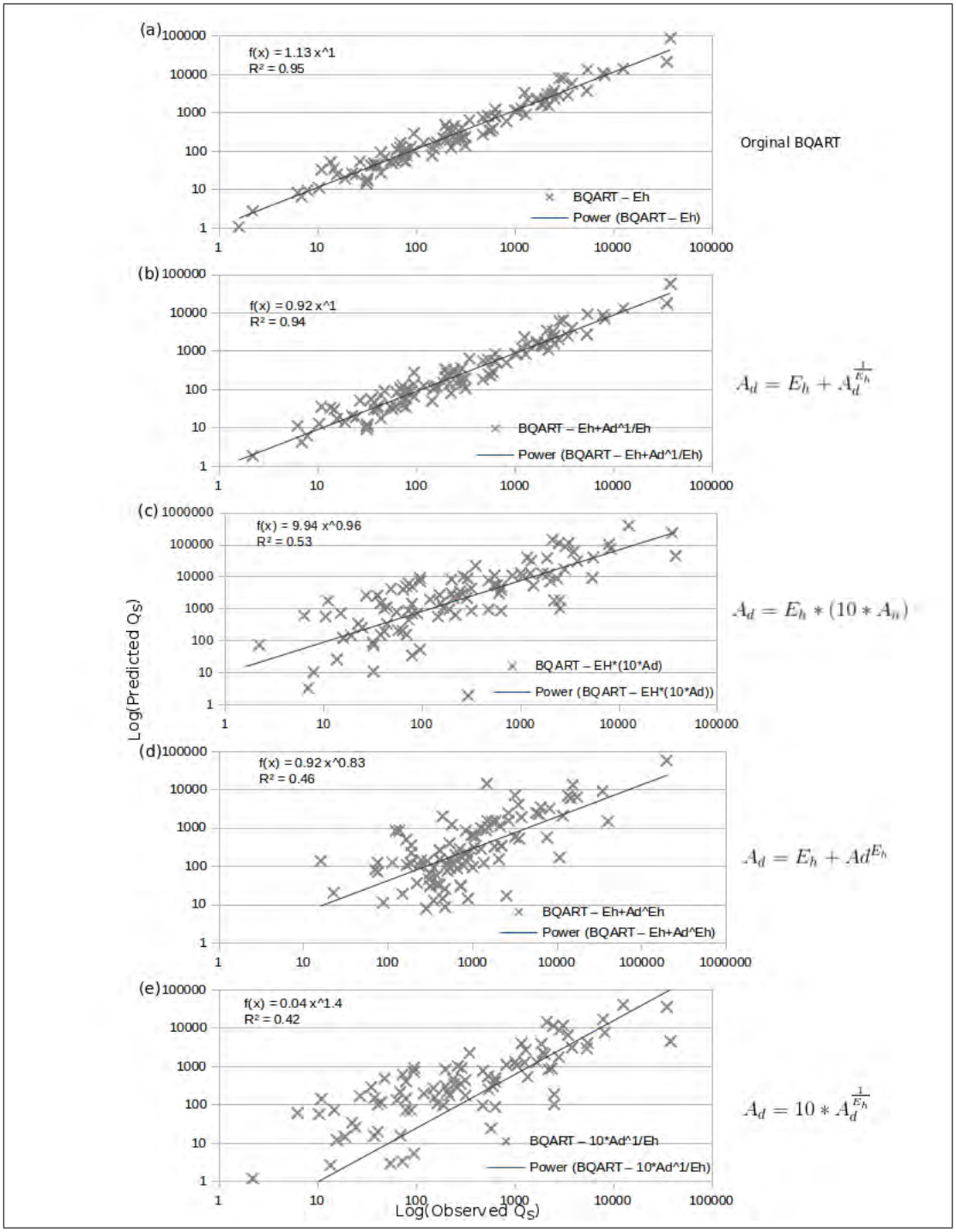

Figure 2.4: Effect of various formulas for A_d on the accuracy of predicted suspended sediment discharge in the BQART equation against the M&S92+ database.

The B equation of the BQART model in WBMsed was therefore modified to:

$$B = IL(1 - T_e)A_d \tag{2.2}$$

2.1.1 Simulation Settings and Validation Data

Following these modifications to the WBMsed source code, the model was run in two simulation modes - first producing results with the A_d variable and the second simulation with the agricultural land-use turned off (A_n set globally to 0). Globally setting A_n to 0 mimics the results of WBMsed prior to the source code modification. Following Cohen et al. (2014), WBMsed was configured to run at 6 arc-minute resolution, outputting monthly and annual predictions. Unlike Cohen et al. (2014) trapping efficiency input files were calculated from the Global Reservoir and Dam (GRanD) database (Lehner et al., 2011).

The simulation results for suspended sediment flux ($\bar{Q}_s$) predictions for years 1980-2010 are averaged and compared with the same files from a WBMsed model run without the A_d variable (i.e. the original model). The $\bar{Q}_s$ files are then compared against 133 river mouths from the M&S92+ database and USGS stream gages. 37 USGS stream gaging stations were selected using the following criteria:

- continuous data collection longer than 10 years overlapping the WBMsed simulation (1980-2010)
- mean discharge greater than 30 m s^{-1}
- USGS catchment area similar to WBMsed catchment area (<10% error)
- no gage was downstream of another gage without the presence of a significant confluence from a tributary

2.1.2 Validation

With the incorporation of the A_d parameter, suspended sediment predictions increased in areas with agriculture, in some places by more than 100% compared with the previous model. This was evident notably in the Midwest portion of the United States, Europe, Southeast and South Asia, and southeast South America (Figure: 2.5).

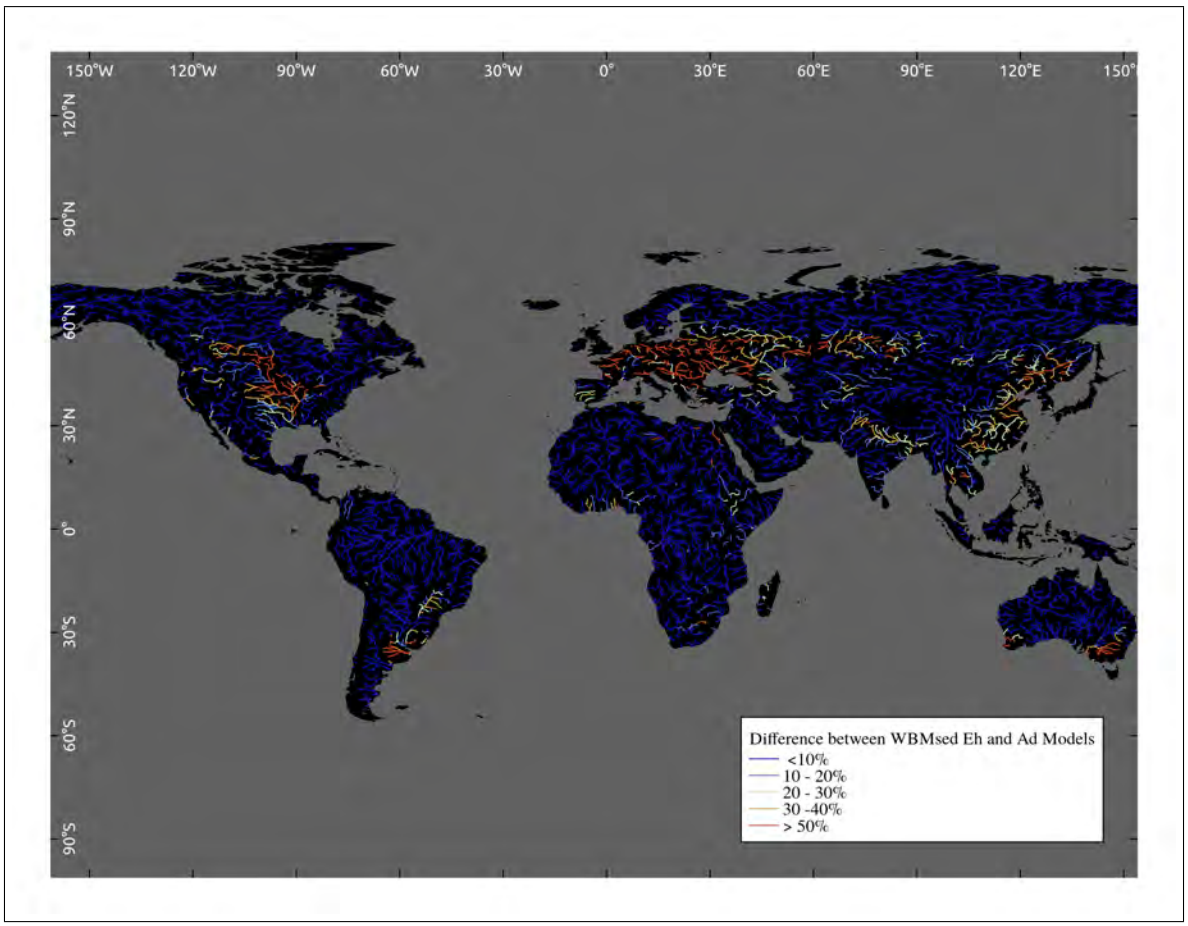

Figure 2.5: Spatial distribution of change of predicted suspended sediment flux using the A_d parameter and original model.

Global model prediction accuracy, however, is relatively unchanged; the coefficient of determination (R^2) = 0.66 versus the previous model's R^2=0.67 when compared against the M&S92+ database river mouths (Figure: 2.6). As expected, differences in suspended sediment increases were limited to smaller basins and the effect of the A_d parameter on suspended sediment predictions generally decreased going downstream. Examination of the A_n files show that A_n values typically decay as a function of increasing catchment area, reflecting the nature of scale and heterogeneity of land-use (Ding et al., 2016).

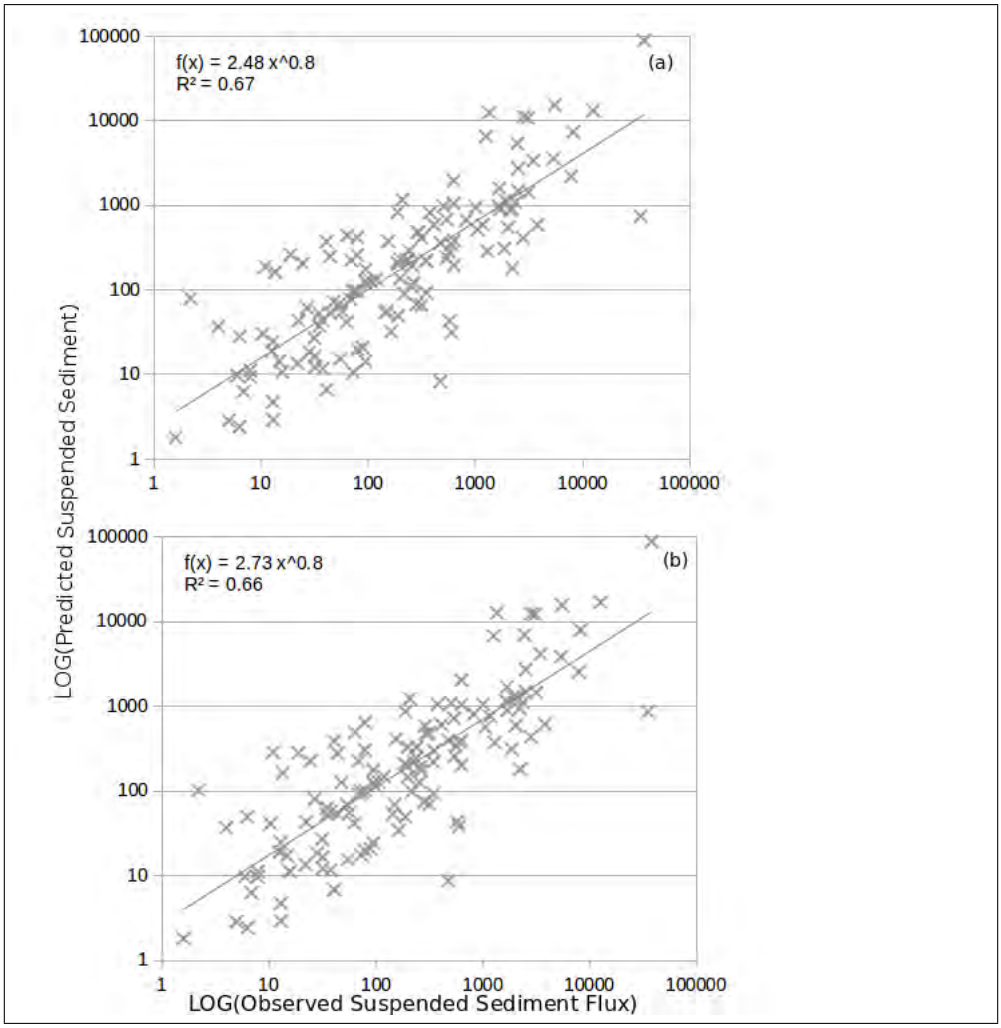

Figure 2.6: Comparison of WBMsed predicted values with (lower figure) and without (upper figure) the A_d parameter against 133 observed long-term mean suspended sediment averages from the M&S92+ database.

WBMsed performance varies spatially across continents. Intra-basin dynamics are present in WBMsed with the A_d parameter. The upper tributaries of the Mississppi River and Nile River show increased suspended sediment flux compared with the original model (Figure: 2.7. Likewise, Europe clearly demonstrates a dichotomy of model predictions between eastern and western Europe. Asian, North and South American modeled sediment quantities correlate well with the M&S92+ database but the model does not perform as well for European and African rivers (Table: 2.1). The disparity of model performance at the continental scale likely stems from the B parameter (Cohen et al., 2013). The most likely cause of model performance degradation in Europe and Africa is calculation of the trapping efficiency variable as most other variables for Europe correlate

well with original BQART calculations (Syvitski and Milliman, 2007).

Table 2.1: Intercontinental WBMsed coefficient of determination of predicted suspended sediment flux versus observed suspended flux (M&S92+ database)

Continent	**WBMsed with A_d**	**WBMsed with E_h**
North America	0.73	0.73
South America	0.71	0.71
Europe	0.34	0.37
Asia	0.73	0.71
Africa	0.30	0.32

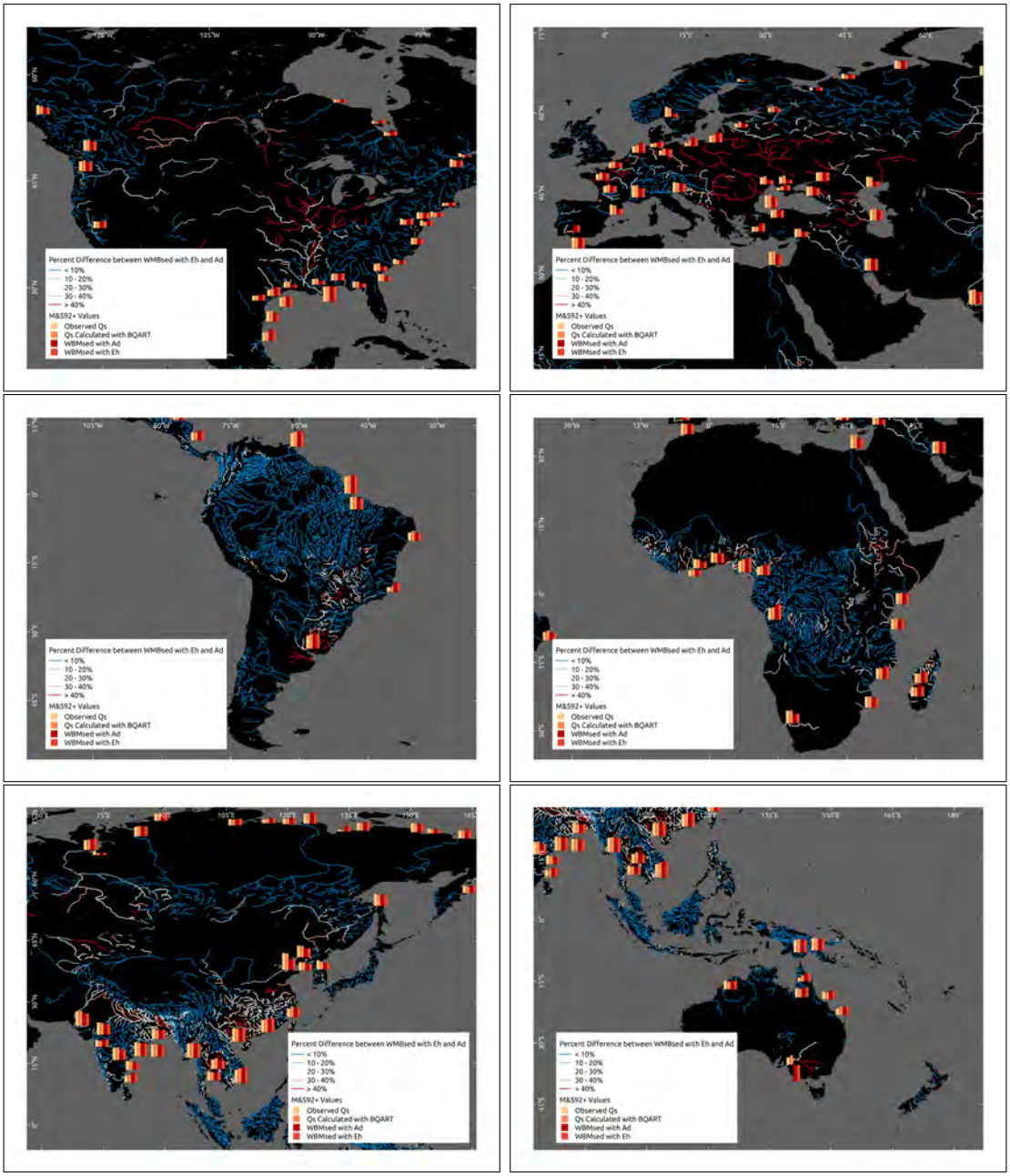

Figure 2.7: Comparison of WBMsed with E_h and A_d at the continental scale.

WBMsed model with the A_d parameter performed slightly better (R^2=0.74 vs R^2=0.73) than with the E_h parameter against the USGS dataset (Table: 2.2). It is notable that WBMsed is now capturing the intra-basin variability caused by the incorporation of the A_d parameter and this is likely cause of increased accuracy on smaller basins.

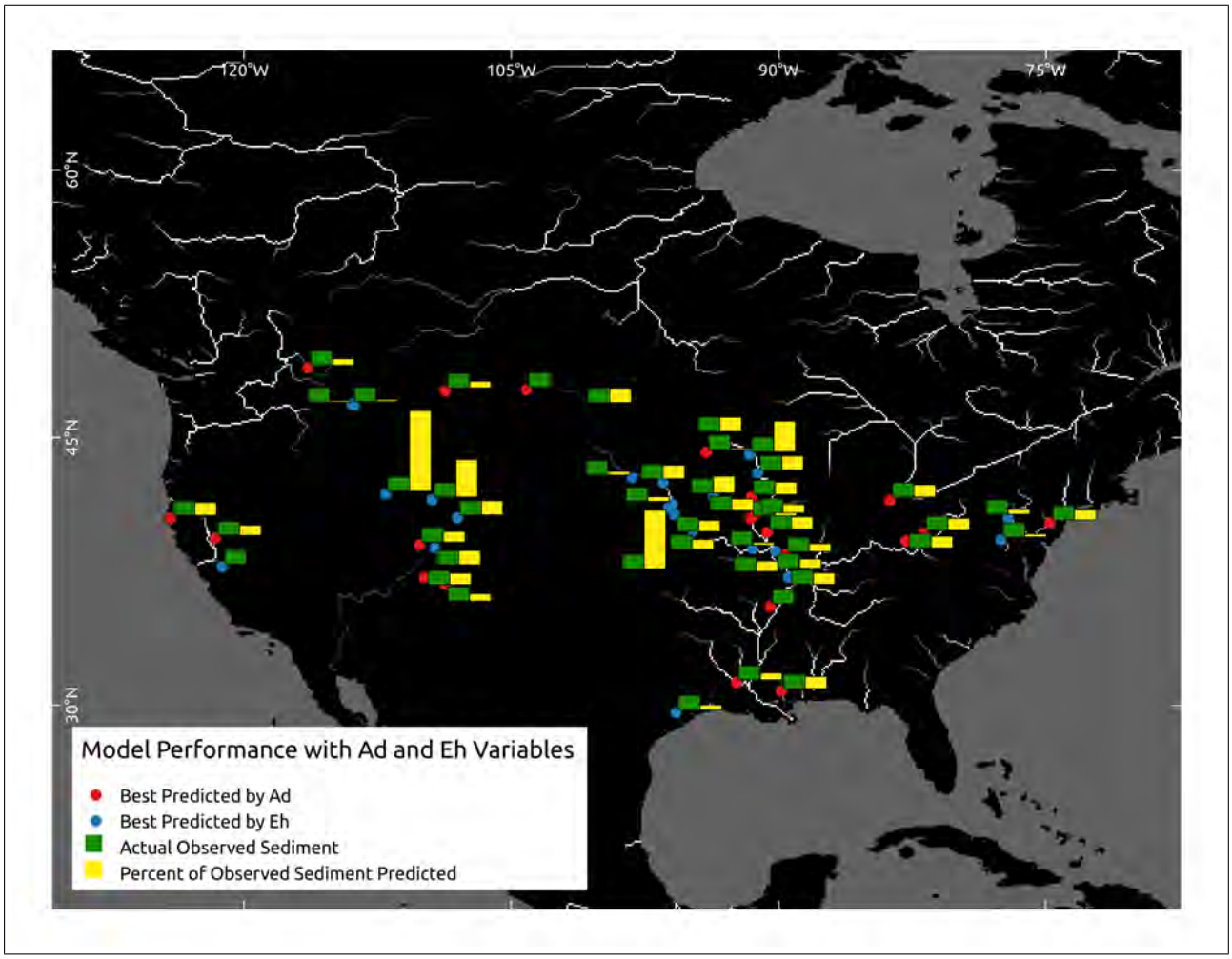

Figure 2.8: Model performance with the A_d parameter evaluated spatially. Yellow bars represent percent difference between WBMsed suspended sediment calculations and observed long-term means. Green bars represent actual suspended sediment flux.

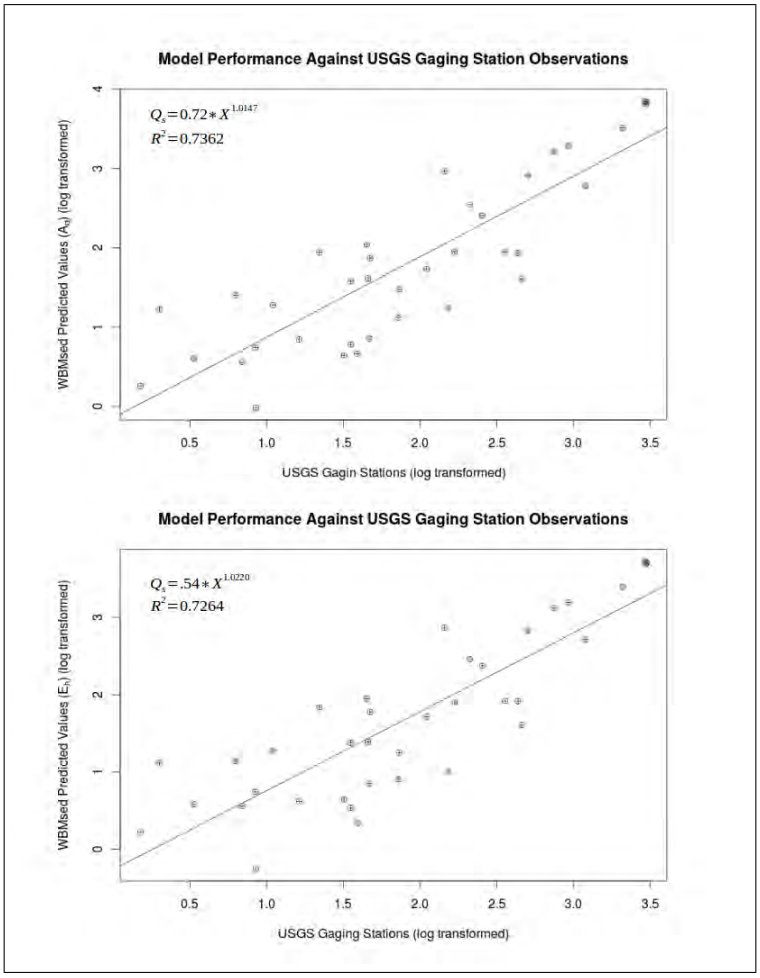

Figure 2.9: Comparison of predicted suspended sediment flux against the observed long-term mean sediment flux at 37 USGS gaging stations.

The relative, albeit small increase in model performance with the A_d parameter in smaller basins (the USGS dataset) is likely the result of scale's influence on factors controlling suspended sediment (i.e. land-use is more important at the smaller scale than larger scales in determining suspended sediment flux). The USGS stream gage data is a more accurate database than M&S92+ and represents intra-basin dynamics that are not captured by M&S92+, so any increase in model performance against the actual observed data is encouraging, although it may not be significantly different. Examining the spatial distribution of the model's accuracy against the 37 USGS gaging stations (Figure: 2.8), it appears that where the A_d parameter is poorly correlated occurs in snow melt dominated river systems (where it over-predicts) and in regions of mixed urban/rural interfaces (where it under-predicts sediment flux) A_d parameter also appears to be more

accurate at station recordings that have relatively low sediment fluxes (Table: 2.2).

Table 2.2: Summary of WBMsed model performance (Q_s (kg s^{-1})) against 37 USGS gaging stations. **Bold indicates more accurate model results.** (USGS, 2016)

USGS Site Name	Observed Q_s	WBMsed Q_s with E_h	WBMsed Q_s with A_d
MINNESOTA RIVER AT MANKATO MN	45.93	24.44	**41.16**
Maumee River at Waterville OH	39.06	2.17	**4.61**
Niobrara River near Verdel Nebr.	47.21	**59.91**	74.05
Des Moines River near Saylorville IA	6.29	**13.75**	25.32
Muskingum River at McConnelsville OH	32.07	4.39	**4.41**
St. Francis River Floodway near Marked Tree AR	35.34	23.91	**37.91**
EEL R A SCOTIA CA	460.28	40.59	**40.80**
Platte River at Louisville Nebr.	144.80	**737.30**	929.35
Clark Fork above Missoula MT	3.36	**3.81**	4.04
Pearl River near Bogalusa LA	46.67	7.15	7.15
Mississippi River at McGregor IA	45.08	**89.01**	110.56
SAN JUAN RIVER AT SHIPROCK NM	110.69	51.95	**54.13**
MISSISSIPPI RIVER AT WINONA MN	22.11	**68.83**	87.44
ILLINOIS RIVER AT VALLEY CITY IL	153.96	10.00	**17.70**
KOOTENAI RIVER NR COPELAND ID	6.93	3.61	**3.63**
Brazos Rv at Richmond TX	211.85	**288.025**	349.39
Skunk River at Augusta IA	72.32	8.02	**13.19**
Iowa River at Wapello IA	73.16	17.74	**30.02**
Missouri River near Landusky MT	168.53	79.63	**89.50**
Yellowstone River near Sidney MT	255.23	237.18	**255.19**
Mississippi River at Thebes IL	2,936.41	**5,304.52**	7,023.74
Mississippi River at Chester IL	3,002.84	**5,140.76**	6,805.73
Mississippi River at St. Louis MO	2,965.50	**4,897.21**	6,475.19
Missouri River at Nebraska City NE	746.414	**1,324.57**	1,624.47
Iowa River at Iowa City IA	8.53	0.56	**0.97**
Missouri River at Hermann MO	2,093.95	**2,505.12**	3,231.66
RED R @ ALEXANDRIA LA	1,202.25	521.49	**607.95**
Clark Fork at Turah Bridge nr Bonner MT	1.51	**1.68**	1.82
SAN JUAN RIVER NEAR BLUFF UT	435.43	82.47	**85.98**
Missouri River at Omaha NE	505.25	**674.97**	818.94
BEAR RIVER NEAR COLLINSTON UT	2.00	**13.20**	16.74
Missouri River at St. Joseph MO	930.46	**1,565.74**	1,943.90
Scioto River at Higby OH	35.38	3.41	**6.052**
Juniata River at Newport PA	8.48	5.52	5.52
KASKASKIA RIVER NEAR VENEDY STATION IL	16.31	4.15	**7.00**
GREEN RIVER AT GREEN RIVER UT	359.91	83.07	**87.65**
Delaware River at Trenton NJ	11.00	19.0	19.0

The addition of the A_d parameter to the BQART equation has the largest effect on

smaller, mostly inland rivers. Overall, its effect is attenuated at scale allowing WBMsed to maintain its accuracy for calculating long-term suspended sediment flux to the coastal ocean. While A_d does not intrinsically improve model accuracy in many streams it does make the model more 'realistic' by predicting suspended sediment that is spatially variable within a basin based on anthropogenic land-use. With all other parameters equal, the A_d parameter allows us a pathway to explore the spatially explicit impact of the agricultural landscape on global suspended flux.

2.2 Quantifying the Effect of Anthropogenic Disturbance on Sediment Flux

Input data used in these simulations follow Cohen et al. (2014) with the addition of the A_d parameter and modified equation for B (Equation: 2.2) in the BQART model. MODIS MCD12Q1 (Friedl et al., 2010) land-use data was processed to create input values for the A_n parameter. To visualize and quantify how suspended sediment flux is altered by anthropogenic disturbance at the global scale, WBMsed is run in three different configurations (Table: 2.3). The first simulation (Model 1 or 'fully disturbed') produces estimated suspended sediment flux representing the current real-world environment (WBMsed variables T_e, E_h, and A_d are calculated). The second simulation (Model 2 or 'isolated anthropogenic disturbance') is configured by setting the T_e parameter to 0 globally, which eliminates sediment trapping in the model, isolating the additive effect of human erosivity and land-use. The third model (Model 3 or 'pristine') is configured to eliminate anthropogenic landscapes ($A_d = 0$, $E_h = 1$, and $T_e = 0$), simulating suspended sediment flux without any human disturbance.

WBMsed is configured for all models using 6 arc-minute resolution inputs following the procedure described in Cohen et al. (2013). The reservoir impoundment database used by Vörösmarty et al. (2003) is limited to impoundments with an operational capacity greater than 0.5km^2. The WBMsed model originally included a separate algorithm for calculating T_e in small reservoirs (described in Cohen et al., 2013). This algorithm was not used in this version of the model as it was found to reduce the model T_e accuracy when

compared to global-scale estimates. By not running the models with the small reservoir storage fraction, we acknowledge that all model outputs will likely underestimate trapping efficiency and over-estimate suspended sediment flux. As this paper is concerned with the long-term $\bar{Q}_s$, the outputs using the Psi variability model which are used for daily time-step simulations were also not used. Model outputs of annual $\bar{Q}_s$ were exported into GIS software and analyzed using common raster math functions. Percent difference was calculated as:

$$\% \; Difference = (x - Pristine)/Pristine \tag{2.3}$$

where x is Model 1 or 2 and Pristine is Model 3 outputs.

Table 2.3: WBMsed parameters run for each simulation

Model	**Parameter**	**Value**
Model 1	E_h	Calculated
	A_d	Calculated
	T_e	Calculated
Model 2	E_h	Calculated
	A_n	Calculated
	T_e	0
Model 3	E_h	1
	A_n	0
	T_e	0

Outputs of the three model runs are post-processed to limit the results to rivers with an annual $\bar{Q}$ of $> 30\ m\ s^{-1}$. Syvitski and Milliman (2007) determined that BQART predictions (which WBMsed is calculating) of streams smaller than $30\ m\ s^{-1}$ were unreliable. WBMsed results were compared against each other and compared at 304 river mouths (Figure: 2.10) from a collected database of river outlets. The river outlet database is limited to rivers with a drainage area >20k km^2. To simplify the analysis of this data, results are analyzed on a per continent basis highlighting large continental draining rivers.

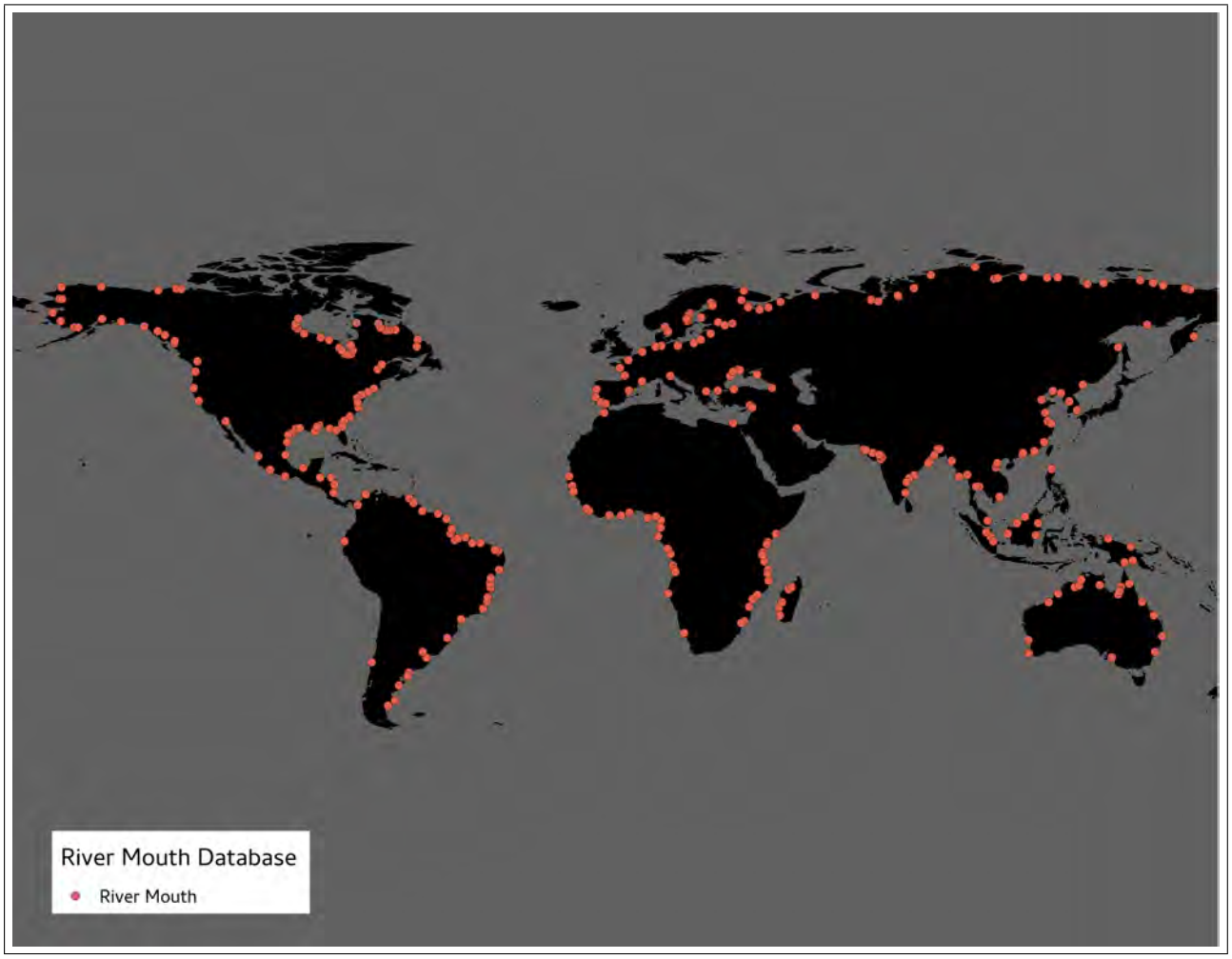

Figure 2.10: Results were compared at 304 river mouths. Combined drainage area represents 55% of global drainage.

CHAPTER 3

RESULTS AND DISCUSSION

3.1 Fully Disturbed Results

At the global scale, anthropogenic disturbances tend to reduce the amount of suspended sediment flux to the coastal ocean. Anthropogenic disturbance can reduce suspended sediment flux in WBMsed through two primary parameters: modern highly urbanized areas (where $E_h = 0.3$) and large reservoirs. Anthropogenic disturbance can increase riverine suspended sediment predictions in areas with agricultural land-use and/or areas in high-population density areas in developing nations. In highly developed areas, such as North America and western Europe, these two factors greatly reduce the amount of modeled suspended sediment. In developing nations, especially in Southeast Asia and Western Africa, the lack of dam construction and expansive areas of impervious surfaces allows disturbed anthropogenic landscapes to increase the suspended sediment flux in rivers compared with 'pristine' conditions.

Averaging the 'fully disturbed' and 'pristine' predictions for the 304 river mouths representing 55% of the continental drainage area (Figure: 2.10), then computing the percent difference between the averages, WBMsed predictions show that anthropogenic disturbance reduce suspended sediment 17%, which closely corresponds to the estimate by Vörösmarty et al. (2003). The effect of anthropogenic disturbance on riverine suspended sediment flux demonstrates inter-continental variability (Table: 3.1). Because all continents demonstrate a reduction of suspended sediment over 'pristine' conditions, the simulations suggest that anthropogenic disturbance on riverine suspended sediment transport to the coastal oceans are dominated by reservoir construction on rivers.

Table 3.1: Intercontinental variation in percent difference between fully disturbed and pristine models 304 river outlets (Figure: 2.10)

Continent	**Percent Difference**	**Number of Outlets**	**Percent of Continental Drainage**
North America	-30%	80	59%
South America	-13%	35	75%
Europe	-52%	50	50%
Africa	-41%	41	51%
Asia	0%	77	52%
Oceania	-22%	19	37%

Examining the model results for North America (Figure: 3.1), the addition of the A_d parameter seems to be overshadowed by the sediment trapping effects of impoundments and reduced sediment production caused by urbanized impervious surfaces. Suspended sediment flux increases occur mainly in smaller tributaries of the Mississippi River in the large agricultural areas of the American Midwest and Canadian province of Alberta. The difference between fully disturbed conditions and pristine conditions (percent difference suspended sediment flux) at the mouth of the Mississippi River indicate a reduction of suspended sediment flux of 11%, which corresponds with an estimated 15% theoretical basin trapping percentage for the Mississippi River provided by Vörösmarty et al. (2003). Figures 3.1-3.3 show the results of the percent difference between the 'fully disturbed' and 'pristine' models. To simplify the data visualization, results were classified as "Increased Sediment" (percent difference >10%), "Unchanged" (percent difference between -10% and 10%), and "Decreased Sediment" (percent difference <10%).

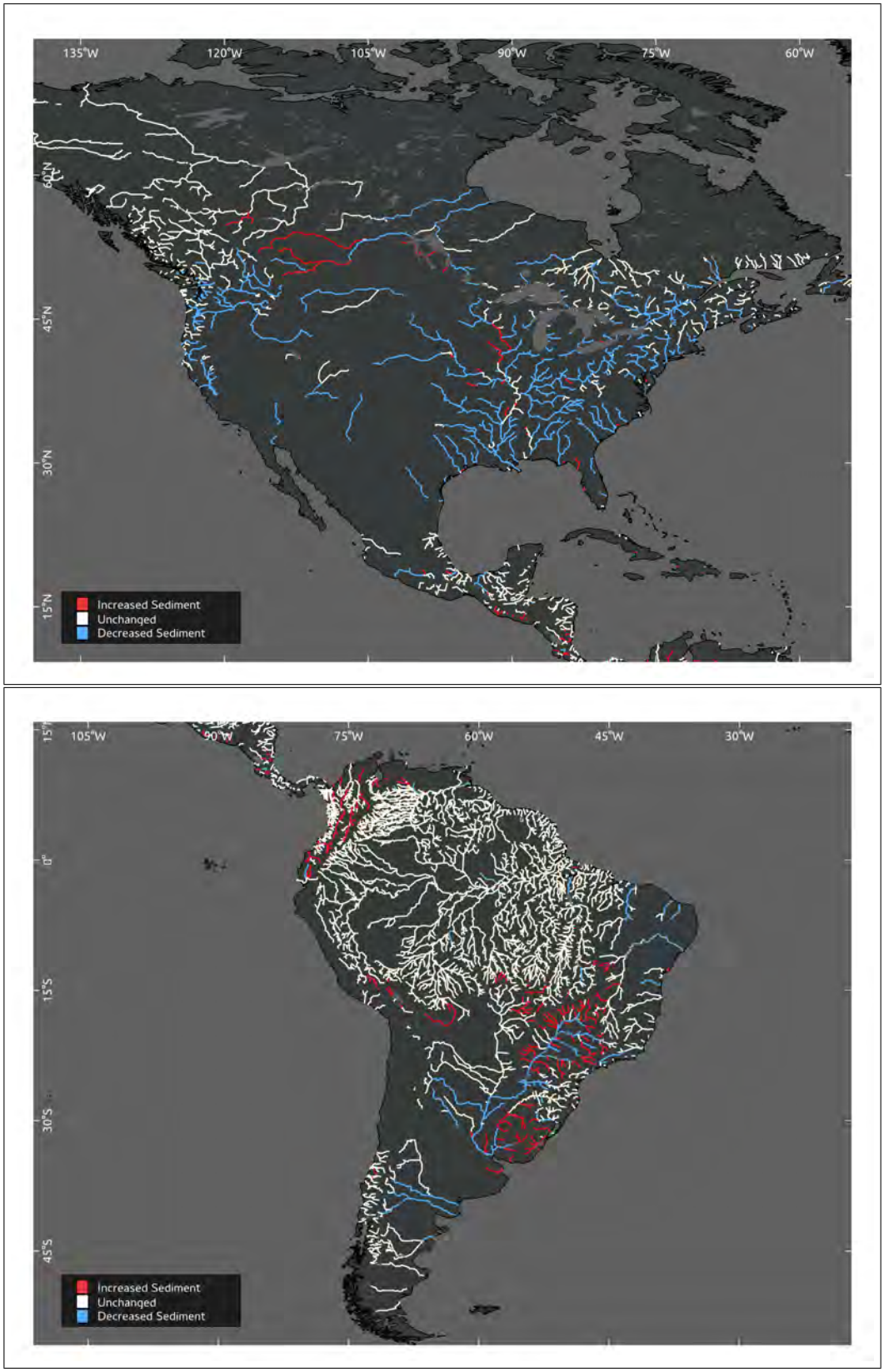

Figure 3.1: Q_s Percent difference between fully disturbed and pristine model conditions for North and South America.

South American rivers (Figure: 3.1) demonstrate more intra-continental diversity in anthropogenic landscape effects on suspended sediment than North America. With the exception of large impoundments in southeastern South America, most of the interior streams of the Amazon River basin are relatively unchanged between fully disturbed and pristine conditions. Anthropogenic landscapes do increase percent difference suspended sediment flux in the southern tributaries of the Amazon and Paraña Rivers in Southern Brazil, Uruguay, and Paraguay, with the greatest increases (>50%) in the agricultural regions of Uruguay and southern Paraguay. Likewise, percent difference suspended sediment flux is increased in the Colombian Valley of Magdalena (east of the Andes Mountains). Anthropogenic landscapes in South America that reduce percent difference suspended sediment flux are caused by hydro-electric dams in eastern South America on the major stems of the Paraña, Uruguay, and Paranaiba Rivers.

Africa (Figure: 3.2) represents a continent of extremes with regard to anthropogenic landscape effects on suspended sediment flux. The mouth of the Nile River demonstrates a 96% reduction of percent difference suspended sediment flux between fully disturbed and pristine conditions; Vörösmarty et al. (2003) estimated the theoretical trapping percentage of the Nile River to be 99%. Rivers of east Africa, however, demonstrate suspended sediment increases well above 100%. The island of Madagascar also demonstrates island-wide suspended sediment increases. Africa's development likely offers key insight into the change of suspended sediment flux regimes' response to changing socioeconomic conditions as nations develop from subsistence agrarian societies to more developed inter-connected societies participating in world trade and industrial scale agriculture (Vanmaercke et al., 2014).

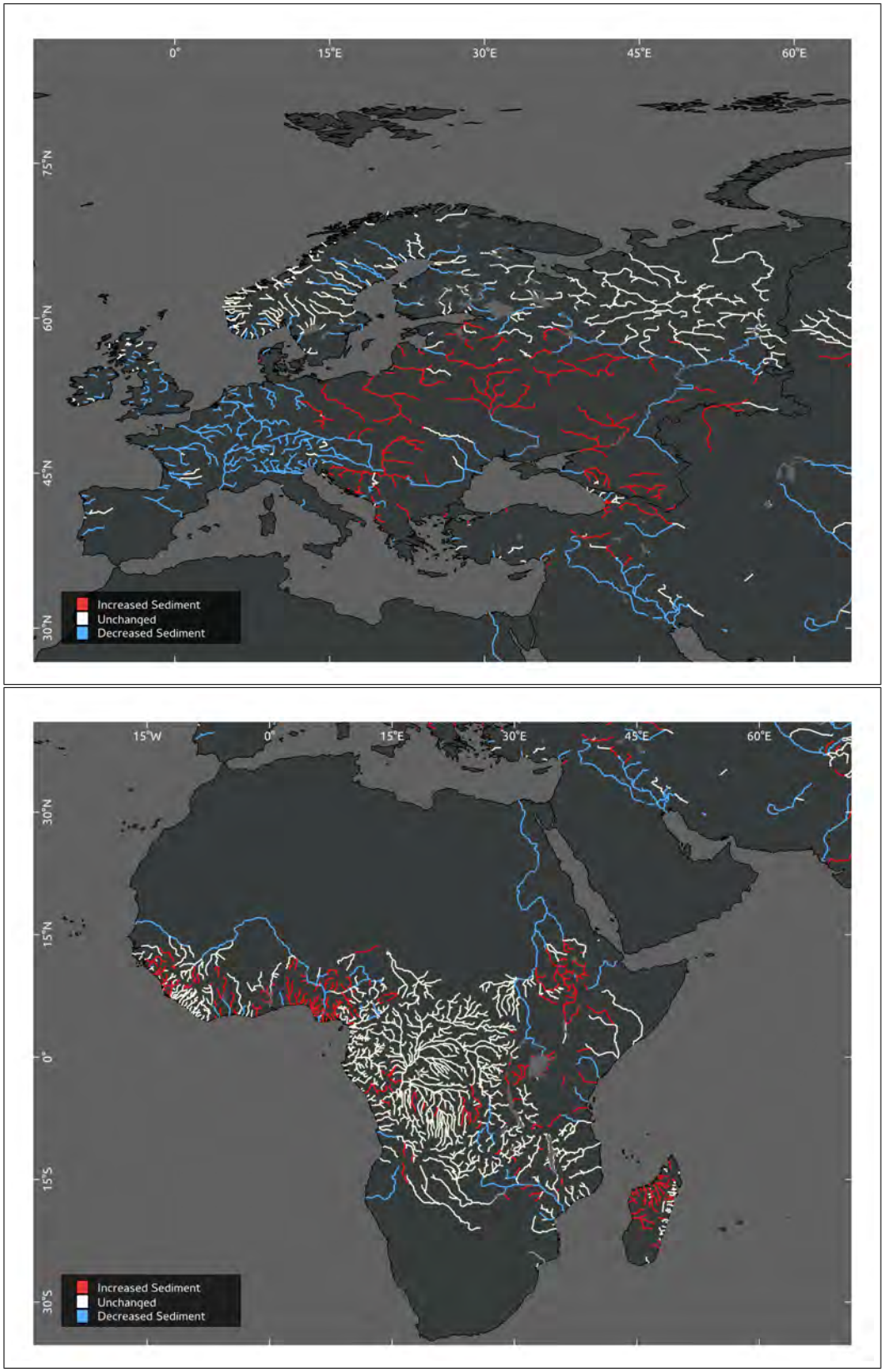

Figure 3.2: Q_s Percent difference between fully disturbed and pristine model conditions for Europe and Africa.

Rivers in Europe (Figure: 3.2) demonstrate how prevailing socioeconomic conditions coupled with recent history control how anthropogenic landscapes affect suspended sediment flux. There is a clear demarcation between eastern and western Europe when examining fully disturbed and pristine conditions. Suspended sediment flux is controlled by dams and impervious surfaces in western Europe whereas, eastern Europe is influenced more by agricultural land-use and sparser populations. Similar to Africa, the land-use change and development of dams and reservoirs in central/eastern Europe will offer insight into how land-use change in the developed nations over the past 50-100 years have modified suspended sediment flux to coastal oceans.

Asian rivers (Figure: 3.3) have much higher (positive) percent difference suspended sediment flux compared with pristine conditions. Asia has the greatest amount of area in WBMsed where E_h=2, which in effect doubles the amount of suspended sediment WBMsed will predict. Coupled with high E_h values are also high A_n values. The A_n variable and attendant A_d parameter are mitigating a chief weakness in WBMsed predictions of Chinese rivers highlighted by Cohen et al. (2014) that as the Chinese economy developed, E_h values abruptly decreased from 2 to 1 reducing suspended sediment flux, which deviates from the calculations of the older M&S92+ database. The Yangtze River is the most significant river in Asia demonstrating suspended sediment flux reduction, with a Q_s percent difference of 84%. This value would be higher if this analysis was limited to years following the Three Gorges Dam initial operating capacity date 2003. The highest concentration of increased suspended sediment in Asia is located on the Indian subcontinent and southeast China. Both areas are dominated by large populations, large agricultural production, and highly erosive soils.

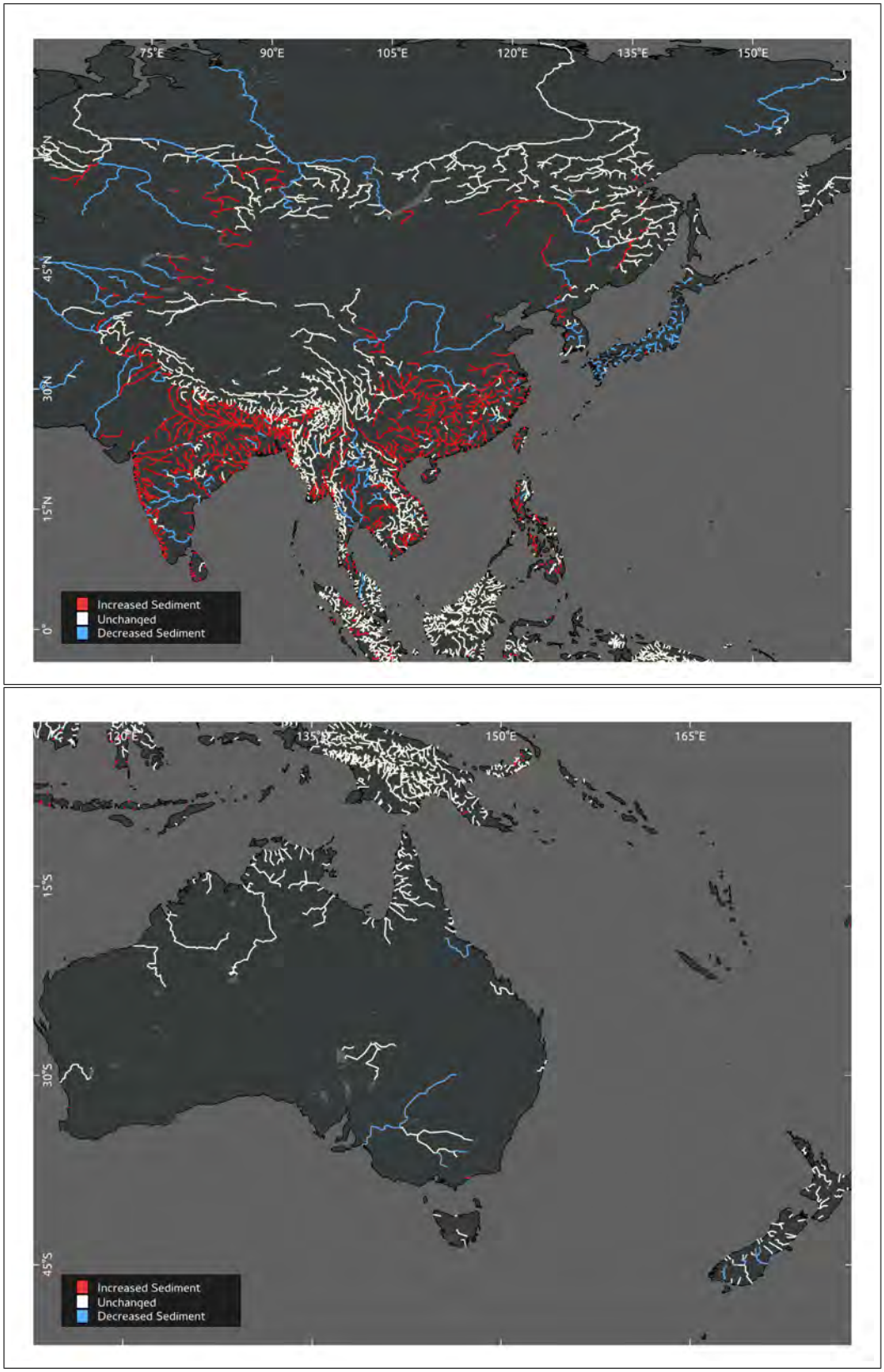

Figure 3.3: Q_s Percent difference between fully disturbed and pristine model conditions for Asia and Oceania

The fully disturbed model shows considerable inter-continental and intra-basin spatial variance of percent difference suspended sediment flux caused by anthropogenic landscapes. With both types of anthropogenic landscapes present in the model (trapping and agricultural disturbance), the presence of dams and reservoirs is the most influential factor determining the flux of sediment from the terrestrial environment to the coastal ocean. Areas where percent difference suspended sediment flux is a positive value tend to occur in developing nations that have yet to begin impounding rivers for reservoirs of drinking water and irrigation or for hydro-electrical power production. To visualize the spatial context and quantity of sediment eroded into streams from agricultural landscapes, we must isolate anthropogenic landscapes that generate additional suspended sediment flux in WBMsed.

3.2 The Effect of Anthopogenic Land-Use

The analysis of this model comparison (Model 2 and Model 3) quantifies the anthropogenic contribution of suspended sediment flux due to anthropogenic disturbance excluding sediment trapping in reservoirs. Results from the comparison of Model 2 and Model 3 suggest that anthropogenic land-use contribute 48% more suspended sediment flux to the coastal ocean. There is considerable inter-continental variation in anthropogenically generated suspended sediment flux with Asia producing the largest percent difference over pristine conditions (Table: 3.2). Asia's large percent difference value is likely due to high E_h and A_n values in key areas.

Table 3.2: Percent difference of sediment without the trapping effects of reservoirs and pristine values at 304 river mouths.

Continent	**Percent Difference**	**Number of Outlets**	**Percent of Continental Drainage**
North America	+23%	80	59%
South America	+8%	35	75%
Africa	+12%	41	51%
Europe	+24%	50	50%
Asia	+114%	77	52%
Ocenia	+9%	19	37%

The effect of land-use disturbance on suspended sediment flux in North America (Figure: 3.4) is mitigated by large areas of highly urbanized areas well inland on both coasts (E_h values of 0.3). In the major cereal agricultural areas of the American Midwest, percent difference suspended sediment flux is increased by over 130% in the northern tributaries of the Mississippi River's Ohio and Northern Mississippi River basins. The increase of percent difference suspended sediment flux over pristine conditions tends to lessen as a function of distance downstream. At the mouth of the Mississippi River, Model 2 predicts 36% more suspended sediment flux compared with pristine conditions. Heterogeneity of landscapes and scale is the likely cause of reduced percent difference of suspended sediment flux predictions in the Mississippi River basin. As area increases so does the number of land-use/land-cover types and landscape heterogeneity (Frazier, 2015), both of which serve to reduce the value of A_n.

WBMsed does not directly calculate the contribution of suspended sediment loads from stream bank erosion. In urban environments, the increased runoff due to impervious surfaces causes smaller streams to widen and deepen in order to carry the increased volume of storm water runoff (Klein, 1979). Suspended sediment flux in streams in North America, especially the large swath of areas calculated with a E_h value of 0.3 in eastern portion of the continent are likely under-estimated. Future development of the WBMsed model should incorporate a stream bank erosion erosion contribution to suspended sediment flux, similar to the SPARROW model (Roman et al., 2012).

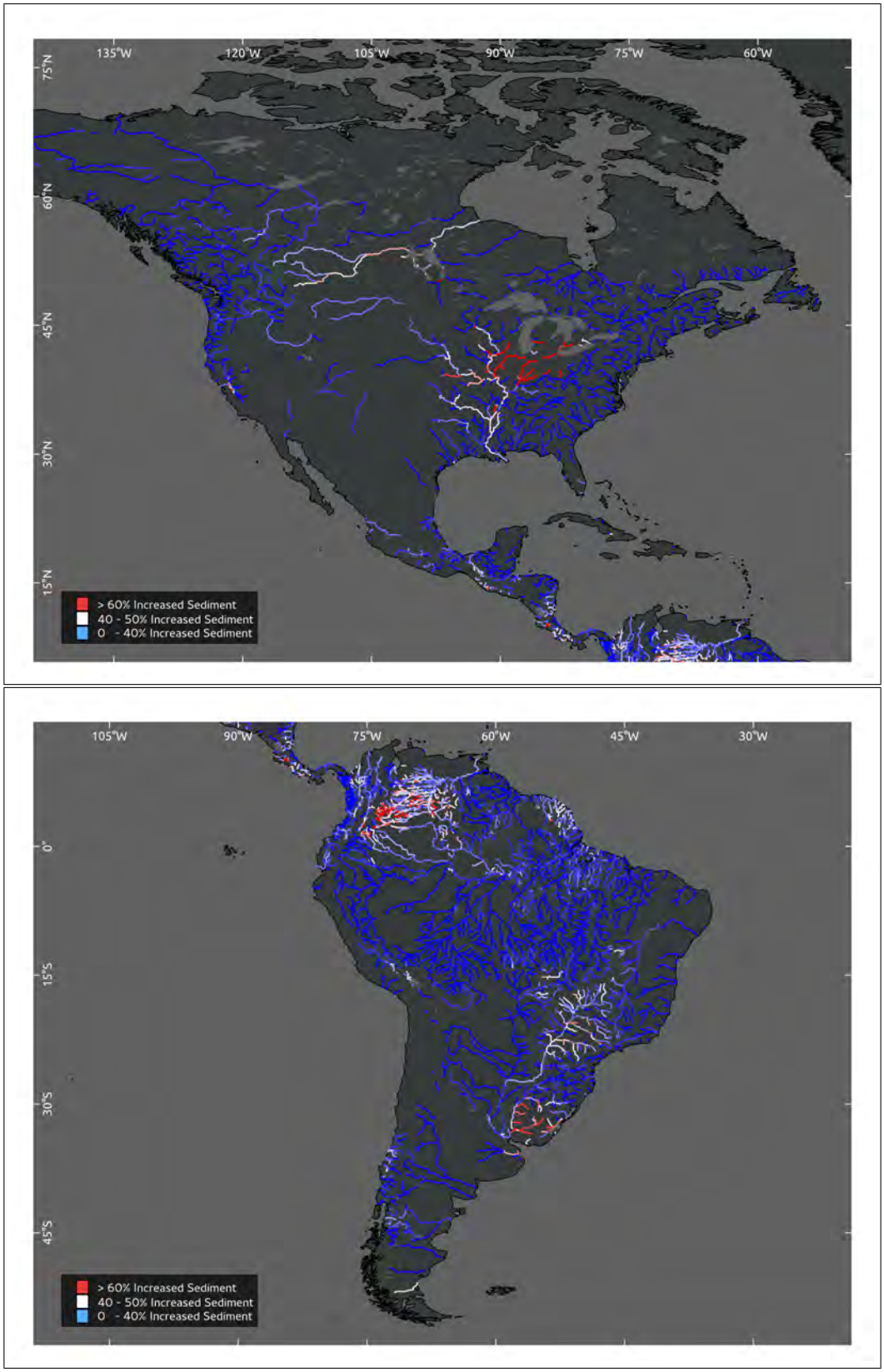

Figure 3.4: Modeled percent difference Q_s without sediment trapping for North and South America.

Land-use in South America (Figure: 3.4) increases suspended sediment flux most significantly in the Orinoco River basin of Venezuela and Colombia. Similar to the predicted results for the Mississippi River, the mouth of Orinoco River has a 36% predicted increase of suspended sediment flux compared with pristine conditions. In the headwaters and smaller tributaries, the WBMsed predictions increase well over 100%. The Paranaiba River and Paraña Rivers maintain significant increases in predicted suspended sediment over pristine conditions by 30%. Unlike North America, urbanization is limited to the coastal regions and urban centers are evaluated to have an E_h value of 2.0. In spite of the increased value of E_h, South American metropolitan areas are situated in such a way that they are insignificant to predicted suspended sediment flux values.

The Nile River in Africa (Figure: 3.5) has a 15% predicted percent difference of suspended sediment flux, which is far lower than the large continental draining rivers in other continents. This is likely caused by the limited areal extent of agriculture in the Nile River basin, where the largest concentration of agriculture lies in the headlands of Ethiopia and the delta region near the mouth of the river. The western African streams of Nigeria, Benin, and Ghana are located in highly urbanized areas co-located with large areas of agriculture. These streams have very high percent difference suspended sediment flux values compared with pristine conditions, with a 30% mean percent difference increase over pristine conditions. Socioeconomic conditions in West Africa are not dissimilar from those in South America and have an E_h=2.0. Unlike South America, however, the urbanized areas of West Africa are sufficiently inland to have an effect on modeled suspended sediment flux.

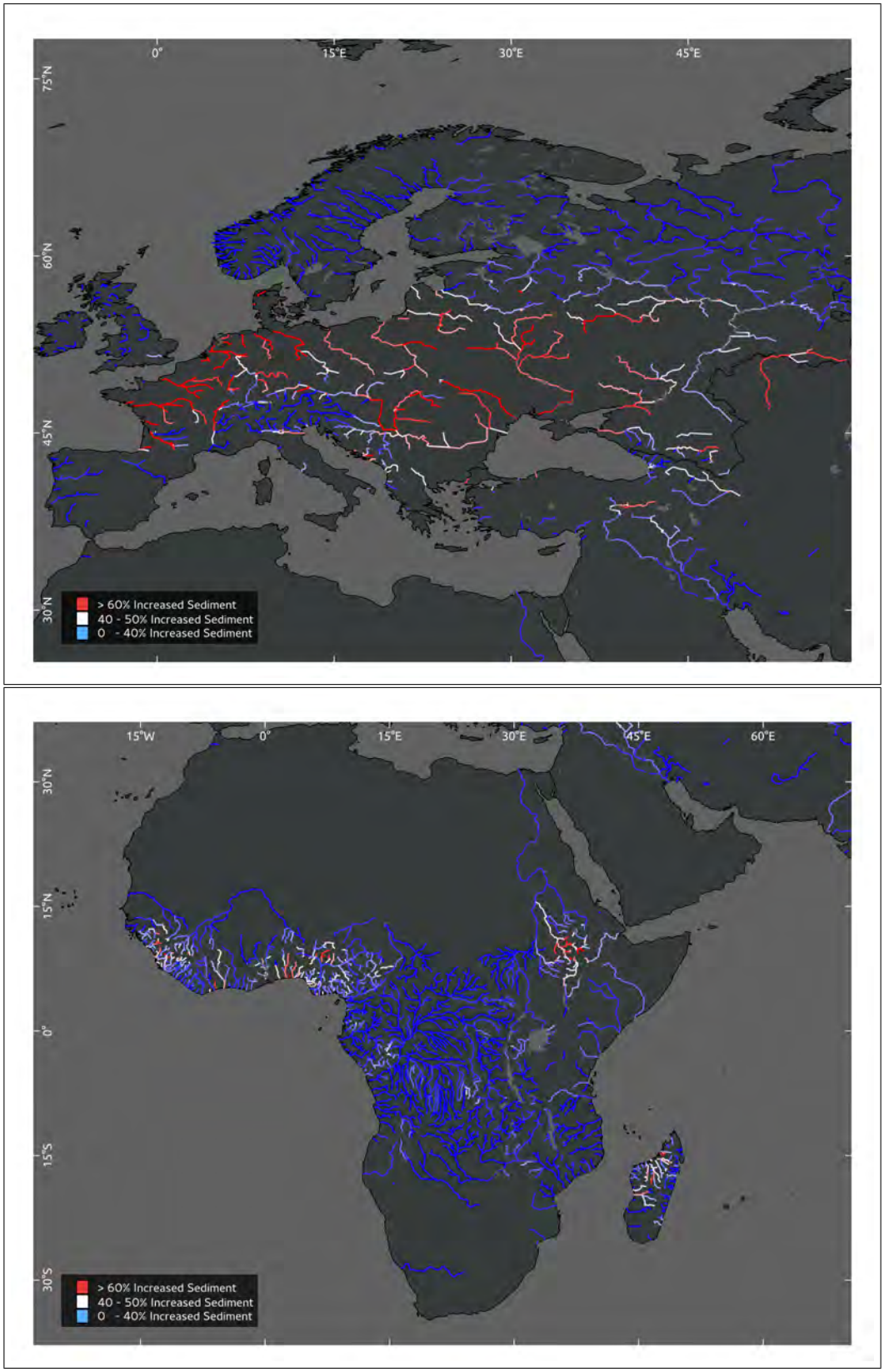

Figure 3.5: Modeled percent difference Q_s without sediment trapping for Europe and Africa.

With the neutralizing effect of reservoirs removed from the model, the increase of suspended sediment flux in European rivers is clearly evident (Figure: 3.5), which is consistent with Ward et al. (2009) analysis that land-cover is the most sensitive factor in predicting suspended sediment in Europe over the past 1,000 years. In spite of the greater amounts of sediment eroded from European topsoils into surface waters, the eroded sediment is not transferred to the coastal ocean, causing continent wide deltaic subsidence since the 1930s (Syvitski and Kettner, 2007). As a continental average, Europe demonstrates the second highest amount of anthropogenic contributions of suspended sediment and the highest amounts of suspended sediment trapping, suggesting that streams in Europe are the most anthropomorphically modified streams in the world.

Rivers in Asia (Figure: 3.6) follow a similar pattern of increased suspended sediment discharge in the isolated anthropogenic disturbance model and fully disturbed model runs. Rivers in the Ganges/Brahmaputra basins and rivers of Southeast China demonstrate the greatest percent difference from pristine. However, in this model run, the rivers of the Indochina peninsula also carry a significant amount of increased sediment. The Yangtze River without the buffering effect of major reservoirs would discharge to the East China Sea more than 35% of natural 'background' sediment. Recent literature suggests that the Yangtze River has undergone steady declines in both water volume and suspended sediment over the past 60 years (Yang and Lu, 2014; Wei et al., 2014). Clearly, land-use and cropping management have had a significant factor in reducing suspended sediment from China's loess plateau, but the overall effect of sediment trapping in reservoirs is significant.

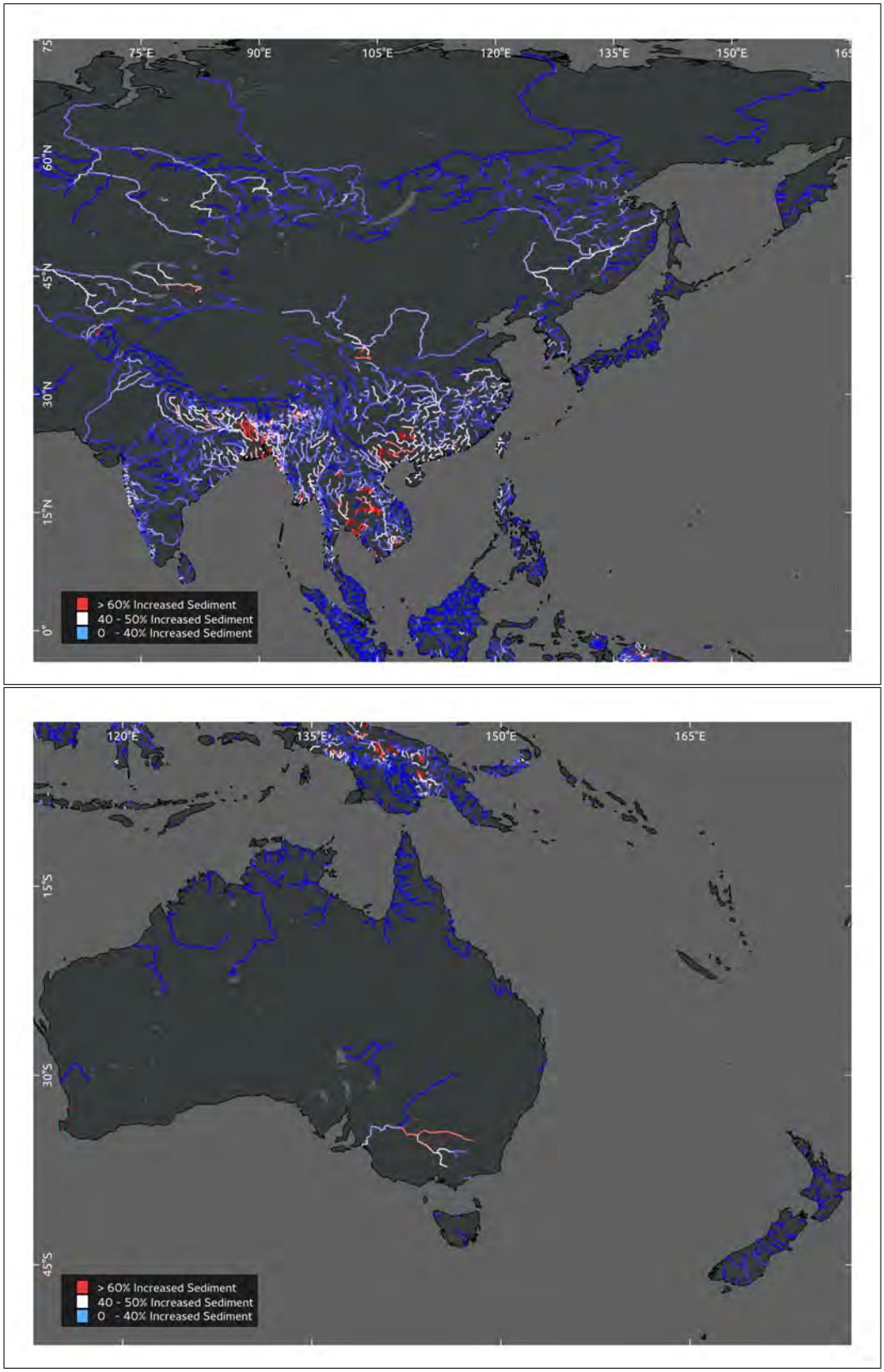

Figure 3.6: Modeled percent difference Q_s without sediment trapping for Asia and Oceania.

Model results in Oceania (Figure: 3.6) are surprisingly low. New Zealand in particular demonstrates percent difference suspended sediment flux of less than 20%. Syvitski and Milliman (2007) highlighted New Zealand as an area where the calculation for the E_h value is not as robust, estimating that many basins in the cattle and sheep herding regions of New Zealand should have E_h values approaching 8. We can safely assume that rivers in New Zealand are significantly under-estimated. In Borneo, the model seems to capture the increases suspended sediment flux we would expect following the deforestation for agriculture in tropical soils (Latrubesse et al., 2005).

CHAPTER 4

CONCLUSIONS

Anthropogenic landscapes modify the suspended sediment flux regime in almost every river. The most significant effect of anthropogenic disturbance is trapping of suspended sediment in large reservoirs. In every river examined in the model, the presence of reservoirs dampen if not eliminate the entire signal of increased suspended sediment flux caused by agricultural land-use. On every continent reservoirs reduce the continental average of suspended sediment flux to the ocean. This is an important signal of human alteration of the transport of sediment from the terrestrial environment to the coastal oceans, resulting in deltaic subsidence (Syvitski and Kettner, 2011; Milliman and Syvitski, 2014). Most striking are the rivers of Asia where anthropogenic disturbance would transfer >114% more suspended sediment to oceans without the trapping effects of reservoirs. With reservoirs, Asian rivers discharge almost the same amount of sediment as pristine conditions. Although anthropogenic land-use creates a greater amount of suspended sediment in Asia, Europe possesses the widest range of percent difference between the fully disturbed and isoloated land-use models. The results of this analysis suggest that the most anthropomorphically modified streams in the world are European streams.

The spatial arraignment of anthropogenic landscapes within basins also appears to be important in determining land-use effects on suspended sediment flux. South American rivers as well as the Nile River in Africa demonstrate a buffered response to anthropogenic landscapes because of the arrangement of the landscapes towards the river mouths. Anthropogenic landscapes towards the upper portion of basins have a much more pronounced affect on suspended sediment effect as seen in the Mississippi, Paraña, and Paraguay Rivers.

Anthropogenic landscapes have greatly accelerated soil erosion throughout most river basins and simultaneously reduced the amount of sediment transported from the terrestrial environment to the ocean. Examined from the perspective of socioeconomic development, agricultural expansion causes an elevated flux of suspended sediment until reservoir development traps sediment and prevents its transport to the coastal ocean. Quantifying the amount of sediment sequestered behind impoundments is important to understanding the amount of soil erosion occurring on the land, an important topic for geomorphologists. As well, the global carbon cycle is intrinsically tied to suspended sediment and sediment burial in the coastal ocean (Worrall et al., 2014).

REFERENCES

Caitcheon, G. G., Olley, J. M., Pantus, F., Hancock, G., and Leslie, C. (2012). The dominant erosion processes supplying fine sediment to three major rivers in tropical Australia, the Daly (NT), Mitchell (Qld) and Flinders (Qld) Rivers. *Geomorphology*, 151-152:188–195.

Cohen, S., Kettner, A. J., and Syvitski, J. P. (2014). Global suspended sediment and water discharge dynamics between 1960 and 2010: Continental trends and intra-basin sensitivity. *Global and Planetary Change*, 115:44–58.

Cohen, S., Kettner, A. J., Syvitski, J. P., and Fekete, B. M. (2013). WBMsed, a distributed global-scale riverine sediment flux model: Model description and validation. *Computers & Geosciences*, 53:80–93.

Ding, J., Jiang, Y., Liu, Q., Hou, Z., Liao, J., Fu, L., and Peng, Q. (2016). Influences of the land use pattern on water quality in low-order streams of the dongjiang river basin, china: A multi-scale analysis. *Science of The Total Environment*, 551552:205 – 216.

Dotterweich, M. (2013). The history of human-induced soil erosion: Geomorphic legacies, early descriptions and research, and the development of soil conservationA global synopsis. *Geomorphology*, 201:1–34.

Flanagan, D., Ascough, J., and Nicks, A. (1995). Overview of the WEPP erosion prediction model. *Water erosion prediction*, (July):1–12.

Flanagan, D. C., Gilley, J. E., and Franti, T. G. (2007). Water Erosion Prediction Project (WEPP): Development History, Model Capabilities and Future Enhancements. *Asabe*, 50(August 1985):1603–1612.

Frazier, A. E. (2015). Landscape heterogeneity and scale considerations for super-resolution mapping. *International Journal of Remote Sensing*, 9(36):2395–2408.

Friedl, M. A., Sulla-Menashe, D., Tan, B., Schneider, A., Ramankutty, N., Sibley, A., and Huang, X. (2010). MODIS Collection 5 global land cover: Algorithm refinements and characterization of new datasets. *Remote Sensing of Environment*, 114(1):168–182.

Hartanto, H., Prabhu, R., Widayat, A. S., and Asdak, C. (2003). Factors affecting runoff and soil erosion: plot-level soil loss monitoring for assessing sustainability of forest management. *Forest Ecology and Management*, 180(1-3):361–374.

Hoffmann, T., Thorndycraft, V., Brown, A., Coulthard, T., Damnati, B., Kale, V., Middelkoop, H., Notebaert, B., and Walling, D. (2010). Human impact on fluvial regimes and sediment flux during the Holocene: Review and future research agenda. *Global and Planetary Change*, 72(3):87–98.

Hunter, H. M. and Walton, R. S. (2008). Land-use effects on fluxes of suspended sediment, nitrogen and phosphorus from a river catchment of the Great Barrier Reef, Australia. *Journal of Hydrology*, 356(1-2):131–146.

Kasai, M., Brierley, G. J., Page, M. J., Marutani, T., and Trustrum, N. a. (2005). Impacts of land use change on patterns of sediment flux in Weraamaia catchment, New Zealand. *Catena*, 64(1):27–60.

Kettner, A. J. and Syvitski, J. P. (2008). Hydrotrend v.3.0: A climate-driven hydrological transport model that simulates discharge and sediment load leaving a river system. *Computers & Geosciences*, 34(10):1170 – 1183. Predictive Modeling in Sediment Transport and Stratigraphy.

Kirkby, M. J. (1980). *Soil Erosion*. J. Wiley.

Klein, R. D. (1979). Urbanization and stream quality impairment1. *JAWRA Journal of the American Water Resources Association*, 15(4):948–963.

Latrubesse, E., Stevaux, J., and Sinha, R. (2005). Tropical rivers. *Geomorphology*, 70(3-4):187–206.

Lehner, B., Reidy Liermann, C., Revenga, C., Vörösmarty, C., Fekete, B., Crouzet, P., Doll, M., Endejan, K., Frenken, J., Magome, C., Nilsson, J., Robertson, R., Rondel, N., Sindorf, N., and Wisser, D. (2011). Global Reservoir and Dam Database, Version 1(GRanDv1): Dams, Revision 01.

Maalim, F. K., Melesse, A. M., Belmont, P., and Gran, K. B. (2013). Modeling the impact of land use changes on runoff and sediment yield in the Le Sueur watershed, Minnesota using GeoWEPP. *Catena*, 107:35–45.

Milliman, J. D. and Syvitski, J. P. M. (2014). Geomorphic / Tectonic Control of Sediment Discharge to the Ocean : The Importance of Small Mountainous Rivers. 100(5):525–544.

Morehead, M. D., Syvitski, J. P., Hutton, E. W., and Peckham, S. D. (2003). Modeling the temporal variability in the flux of sediment from ungauged river basins. *Global and Planetary Change*, 39(1-2):95–110.

Roman, D. C., Vogel, R. M., and Schwarz, G. E. (2012). Regional regression models of watershed suspended-sediment discharge for the eastern United States. *Journal of Hydrology*, 472-473:53–62.

Stolpe, N. B. (2005). A comparison of the RUSLE, EPIC and WEPP erosion models as calibrated to climate and soil of south-central Chile. *Acta Agriculturae Scandinavica, Section B - Soil & Plant Science*, 55(August 2004):2–8.

Syvitski, J. and Kettner, A. J. (2007). On the flux of water and sediment into the Northern Adriatic Sea. *Continental Shelf Research*, 27(3-4):296–308.

Syvitski, J. P. M. and Kettner, A. (2011). Sediment flux and the Anthropocene. *Philosophical transactions. Series A, Mathematical, physical, and engineering sciences*, 369(1938):957–75.

Syvitski, J. P. M. and Milliman, J. D. (2007). Geology , Geography , and Humans Battle for Dominance over the Delivery of Fluvial Sediment to the Coastal Ocean. 115(1):1–19.

USGS (2016). National Water Information System.

USGS, O.-f. (2008). A Preliminary SPARROW Model of Suspended Sediment for the Conterminous United States A Preliminary SPARROW Model of Suspended Sediment for the Conterminous United States.

Vanmaercke, M., Poesen, J., Broeckx, J., and Nyssen, J. (2014). Sediment yield in Africa. *Earth-Science Reviews*, 136:350–368.

Vörösmarty, C. J., Meybeck, M., Fekete, B., Sharma, K., Green, P., and Syvitski, J. P. (2003). Anthropogenic sediment retention: major global impact from registered river impoundments. *Global and Planetary Change*, 39(1-2):169–190.

Walker, J. D., Walter, M., Parlange, J.-Y., Rose, C. W., Meerveld, H. T.-v., Gao, B., and Cohen, A. M. (2007). Reduced raindrop-impact driven soil erosion by infiltration. *Journal of Hydrology*, 342(3-4):331–335.

Walling, D. (2006). Human impact on landocean sediment transfer by the world's rivers. *Geomorphology*, 79(3-4):192–216.

Ward, P. J., van Balen, R. T., Verstraeten, G., Renssen, H., and Vandenberghe, J. (2009). The impact of land use and climate change on late Holocene and future suspended sediment yield of the Meuse catchment. *Geomorphology*, 103(3):389–400.

Wei, W., Chang, Y., and Dai, Z. (2014). Streamflow changes of the Changjiang (Yangtze) River in the recent 60 years: Impacts of the East Asian summer monsoon, ENSO, and human activities. *Quaternary International*, 336:98–107.

Wischmeier, W. and Smith, D. (1965). Predicting Rainfall-Erosion Losses from Cropland East of the Rocky Mountains: Guide for Selection of Practices for Soil and Water Conservation.

Wischmeier, W. and Smith, D. (1978). Predicting rainfall erosion losses: a guide to conservation planning. *U.S. Department of Agriculture Handbook No. 537*, pages 1–69.

Wisser, D., Fekete, B. M., Vörösmarty, C. J., and Schumann, A. H. (2010). Reconstructing 20th century global hydrography: A contribution to the Global Terrestrial Network- Hydrology (GTN-H). *Hydrology and Earth System Sciences*, 14(1):1–24.

Worrall, F., Burt, T. P., and Howden, N. J. (2014). The fluvial flux of particulate organic matter from the UK: Quantifying in-stream losses and carbon sinks. *Journal of Hydrology*, 519:611–625.

Yang, X. and Lu, X. (2014). Estimate of cumulative sediment trapping by multiple reservoirs in large river basins: An example of the Yangtze River basin. *Geomorphology*, 227:49–59.

Zhou, T., Wu, J., and Peng, S. (2012). Assessing the effects of landscape pattern on river water quality at multiple scales: A case study of the Dongjiang River watershed, China. *Ecological Indicators*, 23:166–175.